

## Cerium dioxide nanoparticles as third-generation enzymes (nanozymes)

A. L. Popov<sup>1</sup>, A. B. Shcherbakov<sup>2</sup>, N. M. Zholobak<sup>2</sup>, A. Ye. Baranchikov<sup>3</sup>, V. K. Ivanov<sup>3,\*</sup>

<sup>1</sup>Institute of Theoretical and Experimental Biophysics, Russian Academy of Sciences,  
Pushchino, Moscow region, 142290, Russia

<sup>2</sup>Zabolotny Institute of Microbiology and Virology, National Academy of Sciences of Ukraine,  
Kyiv D0368, Ukraine

<sup>3</sup>Kurnakov Institute of General and Inorganic Chemistry of Russian Academy of Sciences,  
Moscow 119991, Russia

van@igic.ras.ru

PACS 87.55.ne, 87.85.Rs, 81.07.Bc

DOI 10.17586/2220-8054-2017-8-6-760-781

Ceria nanoparticles are capable of performing the function of some enzymes (such as oxidoreductases, phosphatase) and can be classified as nanozymes. In this review, the actual data on the enzymatic activity of ceria were critically analyzed and specific conditions under which the cerium dioxide nanoparticles can act as enzymes were defined. The presented analysis may be useful in the planning, design and synthesis of ceria nanoparticles having the desired enzymatic functions required for various processes, including the development of the nanodrugs, which exhibit the therapeutic effect depending on their composition and pH of media, development of molecular sensors and biosensors, *etc.*

**Keywords:** ceria, nanomaterials, nanozymes, peroxidase, catalase, phosphatase, superoxide dismutase.

*Received:* 24 November 2017

*Revised:* 30 November 2017

### 1. Introduction

It is a well-established fact that almost all biological processes involve enzymes; therefore, the development of the non-proteinaceous analogues of enzymes is among the most interesting and promising tasks in pharmacological and biomedical research. Over the last few decades there have been a series of artificial enzymes created that have replaced the natural ones in a number of practical applications [1–4]. Finally, in very recent years, it has been found that some nanomaterials also exhibit enzymatic activity. Such nanoscale artificial enzymes were called “nanozymes” and were separated into a particular class of biomimetics [5–7]. The diagram (Fig. 1) shows the chronology of the discovery and research of natural and artificial enzymes.

Natural enzymes and well-known industrial inorganic catalysts have a lot of common features. Both natural enzymes and inorganic catalysts are able to increase the rate of chemical reactions; they are also capable of recycling, which means that after the completion of the catalytic cycle the reagents are regenerated to the initial state. Obviously, the previously summarized knowledge of the catalysis and the properties of the catalysts is useful for biomedical applications, including enzyme-mimetic ones.

Generally, the main difference between natural enzymes and technical catalysts is in the rate of the corresponding chemical (biochemical) processes, where the natural enzymes are more active than the artificial ones. However, recent advances in the field of nanomaterials have allowed the creation of catalysts whose characteristics are not inferior to the native enzymes and, in some cases, even surpass them. The natural enzymes, being proteins, are sensitive to reaction conditions and could be inactivated at high temperatures and at a critical pH. The natural enzymes are: 1) highly selective towards the substrate, 2) selective towards the reaction catalysed and 3) stereoselective. The artificial non-proteinaceous analogues of enzymes are attractive due to their low cost, and also because of the wide range of the conditions in which they maintain their activity and stability. Nanozymes are able to operate under harsher conditions, but typically are less selective. The reactions catalysed by nanozymes follow Michaelis-Menten kinetics; however, nanozymes do not satisfy the above-mentioned “triple selectivity” rule. Curiously, some nanozymes can mimic different enzymes, depending on the conditions of the reaction. Thus, the nanoparticles of noble metals and carbon nanotubes are able to exhibit catalase, oxidase and superoxide dismutase activities. Cerium dioxide nanoparticles possess oxidoreductase, phosphatase and possibly NO-reductase activities.

Some metals, semiconductors and insulators are known for their catalytic properties; however, only a small part of them are suitable for *in vivo* biomedical applications. This is caused by the toxicity of nanomaterials, which is determined by several factors, such as the release of their toxic constituents into biological fluids, in molecular or ionic form. The nanoparticles of the transition metal compounds can participate in Fenton/Haber-Weiss reactions,

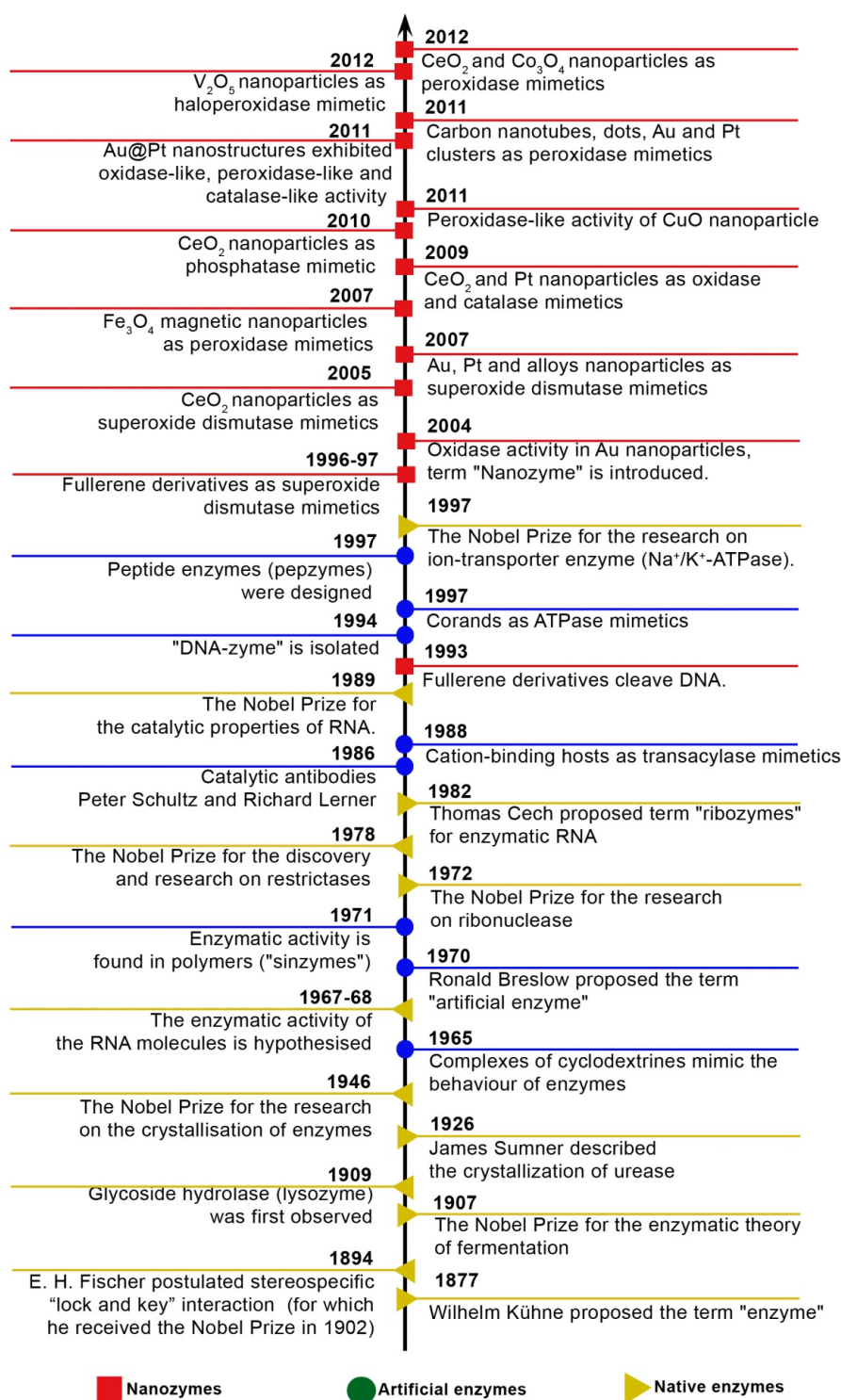


FIG. 1. The chronology of the discovery and research of the three generations of enzymes (adopted from [7])

resulting in the formation of the very toxic hydroxyl radical. Finally, due to their catalytic properties, some of the nanomaterials (oxides of zinc, titanium, cobalt, copper and some other materials, such as carbon nanotubes, etc.) can generate reactive oxygen species (ROS) and cause oxidative stress. This limits the current selection of nanozymes for potential pharmaceutical applications, narrowing it down to the noble metals' nanoparticles (gold, platinum and palladium) and cerium dioxide.

Ceria-based nanomaterials play a key role amongst the currently available nanozymes. The well-known ability of nanoceria to catalyze the redox reactions is widely used in industrial applications (for example, as catalytic converters, reducing harmful emissions in the exhaust fumes from automobiles). Biomedical applications of nanocrystalline cerium dioxide are promising because of two main reasons: its redox activity and its relatively low toxicity. The first factor measures the ability of the cerium dioxide nanoparticle (CDN) to participate in the redox processes in living cells, particularly in the destruction of ROS. The second factor provides that the *in vivo* application of cerium dioxide nanoparticles is safe. One of the key properties of CDNs is the capability of regeneration, which implies that cerium dioxide nanoparticles that have participated in the redox process can return to the initial state over a relatively short period of time.

From the chemical point of view, the dimensional effects are manifested most significantly in the particles where the ratio of surface atoms versus bulk atoms is  $\geq 1$  (which for the octahedral-shaped  $\text{CeO}_2$  particles corresponds to the calculated size of about 4.7 nm (Fig. 2)). In terms of condensed matter physics, the size effects are manifested in the particles of a semiconductor, which are smaller than the Bohr radius of exciton of the corresponding material (for  $\text{CeO}_2$   $\sim 7.0$ – $8.0$  nm [8]). Finally, from the biological point of view, the preferred size of  $\text{CeO}_2$  particles is less than 6 nm, when their cytotoxicity is at the lowest [9]. To date, several methods that would satisfy the denoted criteria have been developed for the synthesis of CDNs, in which the CDNs could form biocompatible sols suitable for nanopharmaceutical applications (some examples are shown in Fig. 3) [10–14]. The conditions of  $\text{CeO}_2$  nanoparticle formation were studied, especially their impact on the characteristics of the formed particles, such as size, degree of crystallinity, oxygen stoichiometry, stability and  $\zeta$ -potential, as well as other parameters that determine the behaviour of the particles in biological systems [9, 15]. The resulting nanoparticles had low toxicity and were able to participate in the reversible redox processes, to protect organic molecules from oxidative degradation. They were also able to inactivate free radicals and had the functionalities of some enzymes.

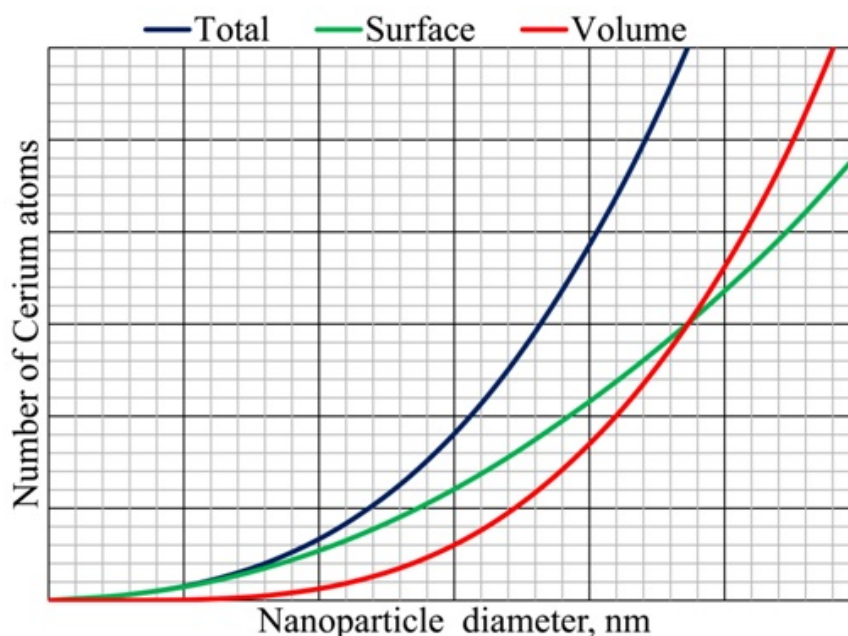


FIG. 2. The calculated number of surface and bulk cerium atoms in  $\text{CeO}_2$  nanoparticles as a function of the particle size. Data for calculation of octahedral-shaped ceria nanocrystal taken from [16]

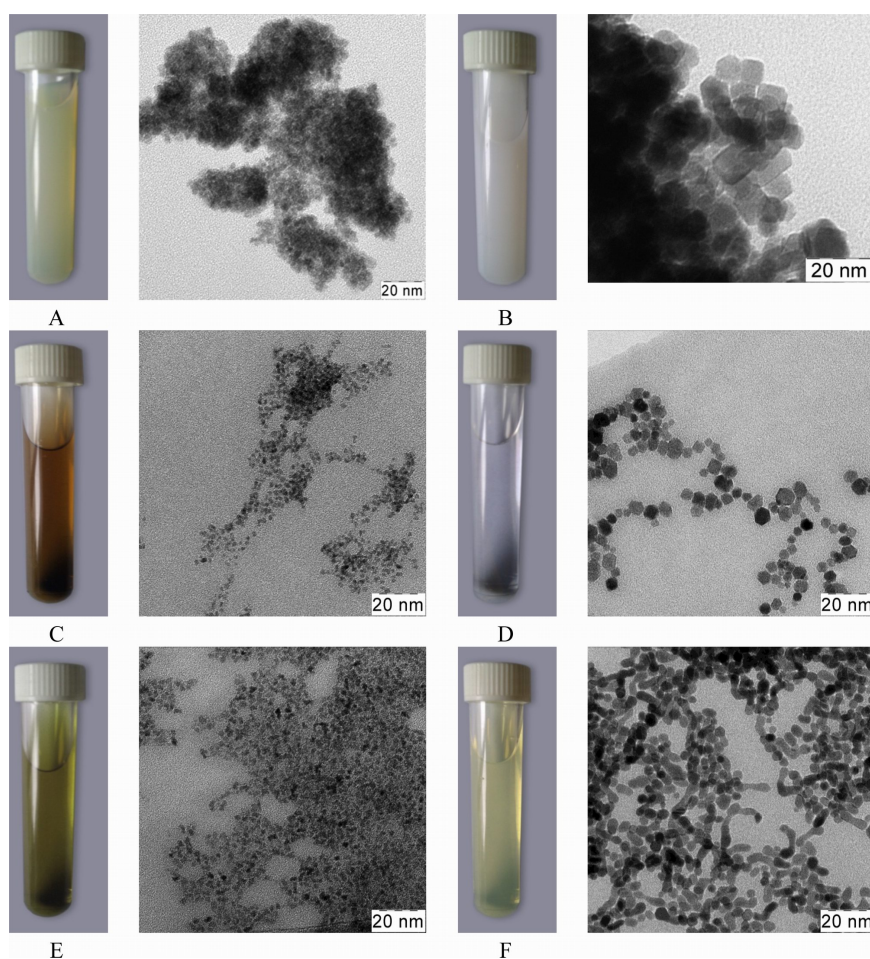
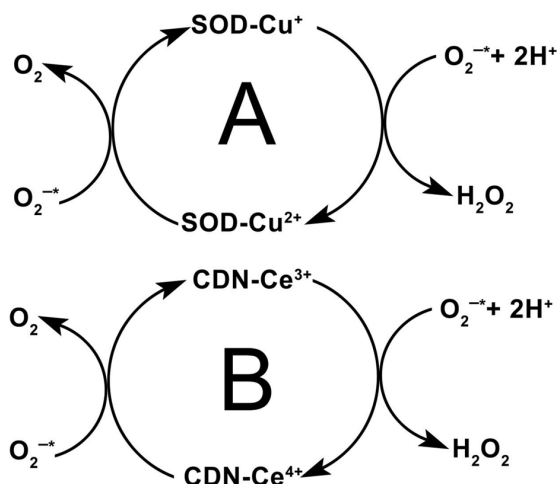


FIG. 3. The appearance and electron micrographs of cerium dioxide samples obtained under various conditions: A – cerium dioxide precipitated from cerium(III) nitrate solution in the mixture of isopropanol:water (19:1) [10], B – sample prepared by microwave hydrothermal treatment at 210 °C for 3 h [10], C – sample prepared by the combination of anionite and microwave-hydrothermal treatments at 190 °C for 3 h [11], D – sample prepared using polyacrylate as stabilizer and further treated hydrothermally at 180 °C for 15 min [12], E – sample prepared using citrate as stabilizer and further treated hydrothermally at 180 °C for 15 min [12], F – sample prepared using citrate as stabilizer and further treated hydrothermally at 180 °C for 3 h [12]

## 2. CDN is superoxide dismutase mimetic

Superoxide radical ( $O_2^{\cdot-}$ ) is one of the most damaging ROS. In cells, superoxide radicals are formed primarily in the mitochondria, where these radicals damage proteins and initiate lipid peroxidation. Protonation of superoxide radicals leads to the formation of even more aggressive hydroperoxyl ( $HO_2^{\cdot}$ ) radicals, reaction with nitric oxide forms peroxynitrite ( $ONO_2^-$ ) radicals. Superoxide radicals destroy iron-sulphur clusters of some enzymes, releasing ferric ions, which are then involved in a Fenton reaction, leading to the formation of hydroxyl radicals ( $OH^{\cdot}$ ).

Superoxide dismutase (SOD) mimetic activity was one of the first discovered enzyme-like functionalities of CDNs [17–20]. For natural SOD and nanoceria, the mechanisms of the reactions with superoxide are similar [20]. It is well known that the inactivation of superoxide anions by superoxide dismutase is a two-stage process: enzymatic radical dismutation leads to the formation of less toxic hydrogen peroxide and oxygen, and then SOD is regenerated. The reaction for copper containing SOD is shown in Scheme 1(A), where the catalyzed reaction is written as follows:  $2O_2^{\cdot-} + 2H^+ \rightarrow H_2O_2 + O_2$ . Nanoparticulate  $CeO_2$  accelerates the same reaction, which includes two stages [20]. After the reaction is completed the effective oxidation state of cerium in  $CeO_2$  remains unchanged; see Scheme 1(B).



Scheme 1. Superoxide dismutase-like activity of CDN

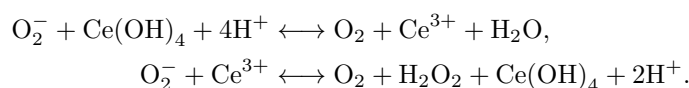
Interestingly, prior treatment of ceria nanoparticles with hydrogen peroxide led to the oxidation of the surface from  $\text{Ce}^{3+}$  to  $\text{Ce}^{4+}$ , which caused the complete loss of superoxide dismutase-like activity in  $\text{CeO}_2$  nanoparticles [18]. However, after a while, the nanoparticles regained the activity, i.e. the particles returned to their original state. These results strongly suggest that the state of the surface of the  $\text{CeO}_2$  particles is important for the inactivation of superoxide radicals, whereas the presence of cerium (III) in the surface layer is the most significant factor. It was also observed that the activity of  $\text{CeO}_2$  nanoparticles, to a great extent, depends on the thickness and permeability of the organic layer of stabilizer on its surface [19].

The ability of the nanosized cerium dioxide to mimic SOD is directly determined by the size factor. Thus, the SOD mimetic activity level of the sample of  $\text{CeO}_2$ , with the particle size of 3–5 nm, was comparable to ferricytochrome C, whereas the sample of  $\text{CeO}_2$  with a larger particle size (5–8 nm) was significantly less active [20].

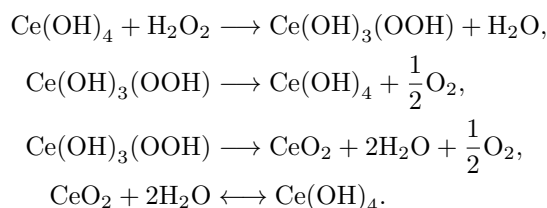
Similarly, epinephrine auto-oxidation in an alkaline medium occurs via the formation of the superoxide radical; nanosized cerium dioxide inhibits this process and the mechanism of the inhibition is similar to that of SOD, whereas the inhibition rate of the process depends on the particle size and pH of the solution [21]. SOD-mimetic activity of CDNs depends on the aggregative stability of sols; it strongly decreases when the threshold of coagulation has been achieved [22].

Batinić-Haberle *et al.* [23] studied a number of SOD-mimetics (manganese compounds, metal nitroxides and oxides, porphyrin and metalloporphyrin derivatives, fullerenes) in detail. It was shown that, among other compounds, SOD-like activity for CDNs (particle size 3–5 nm) had the maximal value, practically at the level of the natural enzyme,  $\log(k_{cat}[\text{O}_2^-]) = 9.55$ . Authors investigated the catalytic dismutation of the superoxide radical from the standpoint of its electrochemical behavior in solution.

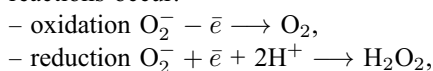
The dismutation of the superoxide radical on the hydrated CDN surface can be written as follows:



The release of hydrogen peroxide leads to the formation and decomposition of cerium hydroperoxide  $\text{Ce}(\text{OH})_3(\text{OOH})$  on the CDN surface:



In practice, on the CDN surface during the dismutation of the superoxide radical, three basic electrochemical reactions occur:



– oxidation-reduction  $\text{Ce}^{3+} + 4\text{H}_2\text{O} \longleftrightarrow \text{Ce}(\text{OH})_4 + 4\text{H}^+ + \text{e}^-$ .

The electrode potential of the superoxide radical dismutation at pH 7.0 in the case of the oxidation reaction is  $E = -0.16$  V, in the case of the reduction reaction is  $E = +0.89$  V (relative to the standard hydrogen electrode) [23,24].

The standard electrode potential of the cerium species in the case of  $\text{Ce}^{3+}/\text{Ce}(\text{OH})_4$  pair is  $E^\circ = +1.97$  V [25]; according to the Nernst equation at pH 7.0:

$$E = 1.97 + 2.3 \frac{RT}{nF} \left( \log \left( \frac{[\text{Ce}(\text{OH})_4]}{[\text{Ce}^{(3+)}]}\right) - 4pH \right) = 0.314 - 0.05916 \cdot \log \left( \frac{[\text{Ce}^{(3+)})]}{[\text{Ce}(\text{OH})_4]} \right).$$

It is obvious that the redox potential essentially depends on the  $[\text{Ce}^{3+}]/[\text{Ce}(\text{OH})_4]$  ratio on the nanoparticle surface.

Figure 4 shows the redox diagram of the reduction and oxidation of a superoxide radical with SOD, as well as the calculated values of the redox potential of stoichiometric and non-stoichiometric CDN at pH 7.0. In the range of 0.2–0.4 V, there is a redox potential of the “ideal”  $\text{O}_2^-$  dismutation catalyst. It can be seen from the figure that CDN is a good redox analogue of SOD, the optimum value of the redox potential is located in the region of a high content of cerium (III) ions when  $[\text{Ce}^{3+}] \approx [\text{Ce}(\text{OH})_4]$  on the surface of the particle.

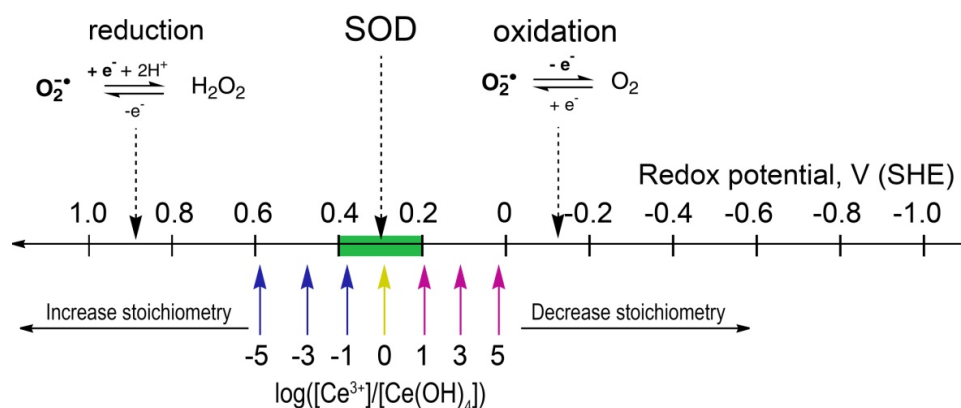


FIG. 4. The diagram of the reduction and oxidation of superoxide radical with SOD (upper part). Green zone shows data for the “ideal”  $\text{O}_2^-$  dismutation catalyst [23,24]. Calculated values of the redox potential of stoichiometric and nonstoichiometric CDN at pH 7.0 (lower part)

This result confirms the authors’ conclusions [18] that cerium dioxide nanoparticles having a high concentration of trivalent cerium possess high SOD-like activity. At the same time, it can be seen from the figure that with increasing  $\text{Ce}^{3+}$  concentration the catalytic activity of the system increases nonlinearly, and after reaching a certain value, its decrease will be observed.

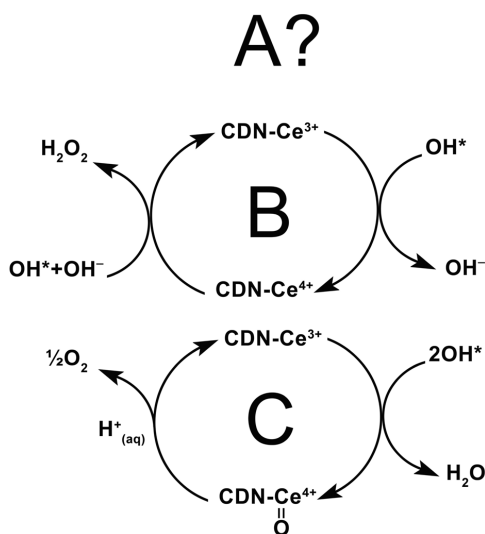
SOD is an anti-oxidant enzyme and plays a vital role in oxidative stress protection systems in most cells which have contact with oxygen. Nanocrystalline cerium dioxide, like SOD, is a powerful protector, enabling the survival of the cells under oxidative stress from exogenous or endogenous ROS.

### 3. CDN can destroy hydroxyl radicals

The hydroxyl radical (OH) is one of the most aggressive ROS: it oxidizes almost all organic molecules – including proteins, nucleic acids and other biopolymers.

This radical is able to tear off hydrogen from molecules of non-saturated fatty acids and to initiate peroxidation of lipids. The specific enzyme, capable of inactivating the hydroxyl radical, is absent in the nature: unlike superoxide, which can be detoxified by superoxide dismutase, the hydroxyl radical is scavenged by molecular antioxidants (vitamin E, ascorbic acid) – but not by an enzymatic reaction, since the hydroxyl radical is extremely reactive and its diffusion to the possible enzyme’s active site is slower than the radical half-life [26]. In the presence of ceria nanoparticles, the blasting activity of the hydroxyl radical decreases, which allows us to assume that CDNs can catalytically destroy OH [15]. In view of the absence of the conforming natural analogue of such a catalyst, it is not obviously possible to define the scheme of the corresponding process (Scheme 2(A)). However, in a pioneering work, the mechanism of interaction of the hydroxyl radical with cerium ions in solution

is described [27]. Possibly, the mechanism of the hydroxyl radical inactivation by cerium dioxide nanoparticles can have a similar appearance (Scheme 2(B)).

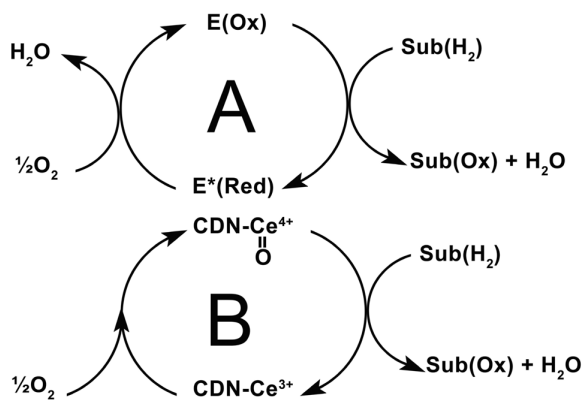


Scheme 2. CDN scavenges the hydroxyl radical

The protective action of CDNs against hydroxyl radical has been confirmed by the data reported: cerium dioxide nanoparticles provided an effective protection for methyl violet dye molecules from the oxidation by hydroxyl radicals, which were formed in Fenton's reaction [28]. The probable mechanism of hydroxyl radical scavenging activity of  $\text{CeO}_2$  nanoparticles was proposed; see Scheme 2(C). It should be noted that the ability of  $\text{CeO}_2$  nanoparticles to inactivate hydroxyl radicals sharply increased with decreasing particles size, which, according to the authors, is due to the increased content of  $\text{Ce}^{3+}$  on the surface of the particle. This pattern was recently confirmed for  $\text{CeO}_2$  nanoparticles stabilized with maltodextrin [29]. The ability of ceria nanoparticles, with the particle size of 3–5 nm, to inactivate superoxide and hydroxyl radicals was also confirmed by EPR [30].

#### 4. CDN is oxidase mimetic

In oxidase-catalyzed reactions, the substrate is oxidized by molecular oxygen, leading to the formation of water, hydrogen peroxide or free oxygen radicals. The mechanism of these reactions is shown in Scheme 3(A) in a simplified form, where  $\text{E}^*(\text{Red})$  and  $\text{E}(\text{Ox})$  are the reduced and oxidized forms of the enzyme.  $\text{Sub}(\text{H}_2)$  and  $\text{Sub}(\text{Ox})$  are the reduced and oxidized forms of the substrate respectively. CDN is shown to possess catalase-like activity; for instance, at low pH, the dextran-stabilized  $\text{CeO}_2$  nanoparticles could oxidize the organic dyes, such as 3,3,5,5'-tetramethylbenzidine and 2,2-azinobis(3-ethylbenzothiazoline-6-sulfonic acid), as was reported [31]. The authors demonstrate that oxidase-mimetic properties of CDNs could be used in immunoassays, including those for identification of cancer cells. The most plausible mechanism of the oxidase-like activity of CDNs is shown in Scheme 3(B), which is similar to Scheme 3(A) [31].



Scheme 3. Oxidase-like activity of CDN

According to the Pourbaix diagram for cerium, upon decreasing pH, the oxidizing ability of  $\text{Ce}^{4+}$  is enhanced and the reaction rate under Scheme 3(B, right part) increases, while the possibility of particles' regeneration under Scheme 3 (B, left part) drops. Probably, CDNs exhibit maximal oxidase-like activity at certain pH in the acidic domain.

The concentrations of quadrivalent (as  $\text{CeO}_2$ ) and trivalent cerium ions in aqueous media are linked by the equation [25]

$$\log(\text{Ce}_{\text{CeO}_2}^{4+}/\text{Ce}^{3+}) = 3\text{pH} - 7.288 + \frac{1}{4} \log(p_{\text{O}_2}).$$

At atmospheric pressure ( $p_{\text{O}_2} = 0.2$ ),  $\text{Ce}_{\text{CeO}_2}^{4+}$  is equal to  $\text{Ce}^{3+}$  at  $\text{pH} \approx 2.5$ ; at pH 2 only approximately 1 % of  $\text{Ce}^{3+}$  ions in  $\text{CeO}_2$  can be oxidized by the dissolved oxygen to  $\text{Ce}^{4+}$  [25]. Moreover, at low pH values, especially in the presence of acids capable of forming complexes with cerium ions (citric, ethylenediaminetetraacetic, etc.), after the stage of substrate oxidation (Scheme 3(B), on the right),  $\text{CeO}_2$  nanoparticles can even dissolve [32]. However, over time (especially upon the increasing of pH)  $\text{Ce}^{3+}$  ions can be re-oxidized by the dissolved oxygen, forming  $\text{CeO}_2$  nanoparticles again (see Figs. 5,6). For instance, at pH=5 the equilibrium ratio of  $\text{Ce}_{\text{CeO}_2}^{4+}/\text{Ce}^{3+}$  concentrations is ca.  $3 \cdot 10^7$ , i.e. there are practically no free  $\text{Ce}^{3+}$  ions in the solution.

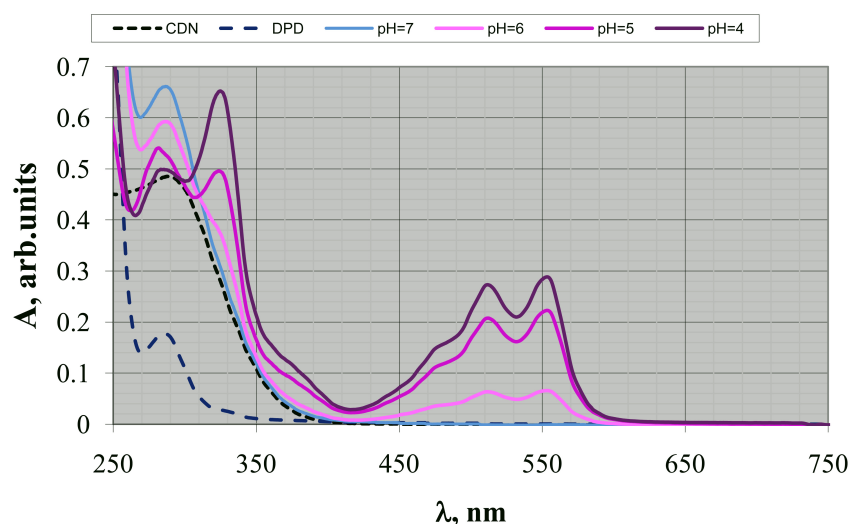


FIG. 5. Absorption spectra of 0.1 mM ceria sol (particle size 3–5 nm, stabilized by citrate,  $\zeta$ -potential  $-20$  mV), 0.1 mM solution of N,N-diethyl-p-phenylenediamine (DPD) and their mixture upon 5 min exposition at different pH

Oxidase-like activity of CDNs does not depend on the presence of small ions in solution (including acetate or citrate); however, DNA adsorption completely eliminates this enzymatic activity, restricting substrate access to the surface of nanoceria [33].

## 5. CDN is catalase mimetic

Hydrogen peroxide ( $\text{H}_2\text{O}_2$ ) is one of the most important ROS in a cell. In catalase-catalyzed reactions, hydrogen peroxide is a substrate that is decomposed into non-toxic constituents (water and oxygen) in the presence of the enzyme. Catalase (as well as glutathione peroxidase) is the enzymatic component of the primary antioxidant system of the cell's protection. The well-known mechanism of catalase action is shown in Scheme 4(A). The commonly accepted mechanism of CDNs' catalase-like activity is shown in Scheme 4(B). However, this scheme is not fully correct, because the process of hydrogen peroxide decomposition in the presence of nanoceria is more complex and actually proceeds in several stages 4(C).



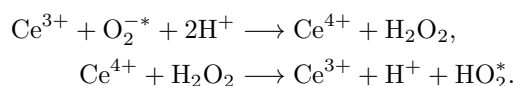
At the first stage, the trivalent cerium ions on the surface of CDNs are oxidized by hydrogen peroxide to  $\text{Ce}^{4+}$  (Scheme 4(C1, right)). Simultaneously,  $\text{H}_2\text{O}_2$  is irreversibly bonded to  $\text{Ce}^{4+}$  ions on the surface of nanoceria, forming cerium perhydroxide (Scheme 4(C2, right)) [34]; in turn, cerium perhydroxide further decomposes with oxygen formation (Scheme 4(C2, left)). The presence of hydroxyl groups on the surface of  $\text{CeO}_2$  particles considerably facilitates the formation of perhydroxide (see Scheme 4(C)). For this reason, ceria sols obtained using “soft chemistry” methods in mild conditions show enhanced catalase mimetic activity, while for well-annealed ceria particles this ability is suppressed or nearly absent [35].

Typically, the injection of  $\text{H}_2\text{O}_2$  decreases the aggregative stability of ceria sols. Hydrogen peroxide is strongly adsorbed on the surface of cerium dioxide nanoparticles, displacing inorganic or organic ligands (stabilizers, dyes etc.).

The mechanism of perhydroxide decomposition on a surface of CDN is not clear yet. In the case of aqueous solutions of cerium salts, the formation of hydroxyl and superoxide (hydroperoxyl) radicals as intermediates is assumed [36, 37]; it was established that decomposition of hydrogen peroxide by cerium (III) ions occurs via Fenton/Haber-Weiss mechanisms [38]. However, in the case of cerium dioxide nanoparticles, these free radicals either cannot be formed or decay at the moment of their formation, according to Schemes 1 and 2. The ability to decompose  $\text{H}_2\text{O}_2$  without releasing the aforementioned harmful oxygen radicals is a specific feature of cerium dioxide nanoparticles that distinguishes CDNs from both cerium salts and most other metal oxides (including nanocrystalline ones). Due to the catalase-like activity of CDNs, the free hydrogen peroxide cannot be released in SOD-mimetic (Scheme 1(B)) or hydroxyl radical scavenging (Scheme 2(B)) cycles because  $\text{H}_2\text{O}_2$  is immediately decomposed by  $\text{CeO}_2$ , according to Scheme 4(C). Cerium perhydroxide formation was observed during the interaction of cerium compounds and  $\text{O}_2$ -radicals [39].

To estimate the contribution of the C1 process into the mechanism of hydrogen peroxide decomposition by cerium dioxide nanoparticles, it is useful to analyze the redox behavior of  $\text{H}_2\text{O}_2$  and cerium species in aqueous systems (see below). On the other hand, it was demonstrated that the catalase mimetic property of CDNs (unlike the SOD mimetic one) essentially depends on the content of quadrivalent cerium in a particle [40, 41]. Therefore, it is possible to assume that the C2 cycle introduces an appreciable (or even the major) contribution to the catalytic decomposition of hydrogen peroxide by cerium dioxide nanoparticles.

Das *et al.* [41] proposed the mechanism of  $\text{H}_2\text{O}_2$  decomposition by tetravalent cerium ion as a part of the ROS-scavenging cycle of CDNs in a biological tissue:



According to the Pourbaix diagram, hydrogen peroxide reduces ceric ions in acidic media. Probably, the proposed scheme explains pro-oxidant properties of CDNs under acidic conditions, because thus forming hydroperoxyl radicals is more aggressive than both the starting superoxide radicals and intermediate hydrogen peroxide.

The formation and decomposition of the dark-colored cerium perhydroxide led to the common misconception that visual changes of the  $\text{CeO}_2$  sol's color occur due to the oxidation and reduction of cerium ions in ceria particles. Fig. 7 shows the changes in the absorption spectra and the color of  $(\text{NH}_4)_2\text{Ce}(\text{NO}_3)_6$  aqueous solution upon peroxide injection. Surely,  $\text{Ce}^{4+}$  ions cannot be further oxidized; nevertheless, the solution becomes deeply colored. In turn, the addition of hydrogen peroxide to an aqueous cerium (III) nitrate solution doesn't lead to an immediate change of color.

The absorption spectra of ceria aqueous sols before the injection of hydrogen peroxide and during several cycles of decomposition at different pH are presented in Fig. 8.

One can see that a decrease in pH decreases the intensity of the sols' coloration caused by  $\text{CeO}_2$  interaction with hydrogen peroxide, which indicates slowdown of C1 and C2 (right) stages. The kinetics of interaction is shown in Fig. 9. The duration of a single redox-cycle (formation and decomposition of cerium perhydroxide) only slightly depends on a ratio of concentrations of ceria nanoparticles and  $\text{H}_2\text{O}_2$ , and strongly depends on the pH of the solution. The rate of formation of cerium perhydroxide and the decomposition of hydrogen peroxide decreases abruptly with a decrease in pH. For aqueous ionic cerium complexes, the rate of  $\text{H}_2\text{O}_2$  disproportionation at  $t = 25^\circ\text{C}$  and  $\text{pH} \rightarrow 5.0$  drops practically to zero [37]. The available data shows that the catalase-like activity of nanoceria also depends on the pH of the solution (catalase activity increases with the pH of the solution and decreases with the decrease of the pH) [42].

## 6. CDN as peroxidase mimetic and the interplay of CDN's pro-oxidant and anti-oxidant properties

The ability of CDNs to catalyze the oxidation of organic molecules by hydrogen peroxide in an acidic medium (peroxidase activity) was observed, e.g. in the reaction of  $\text{H}_2\text{O}_2$  with bioflavonoids (e.g. anthocyanins of

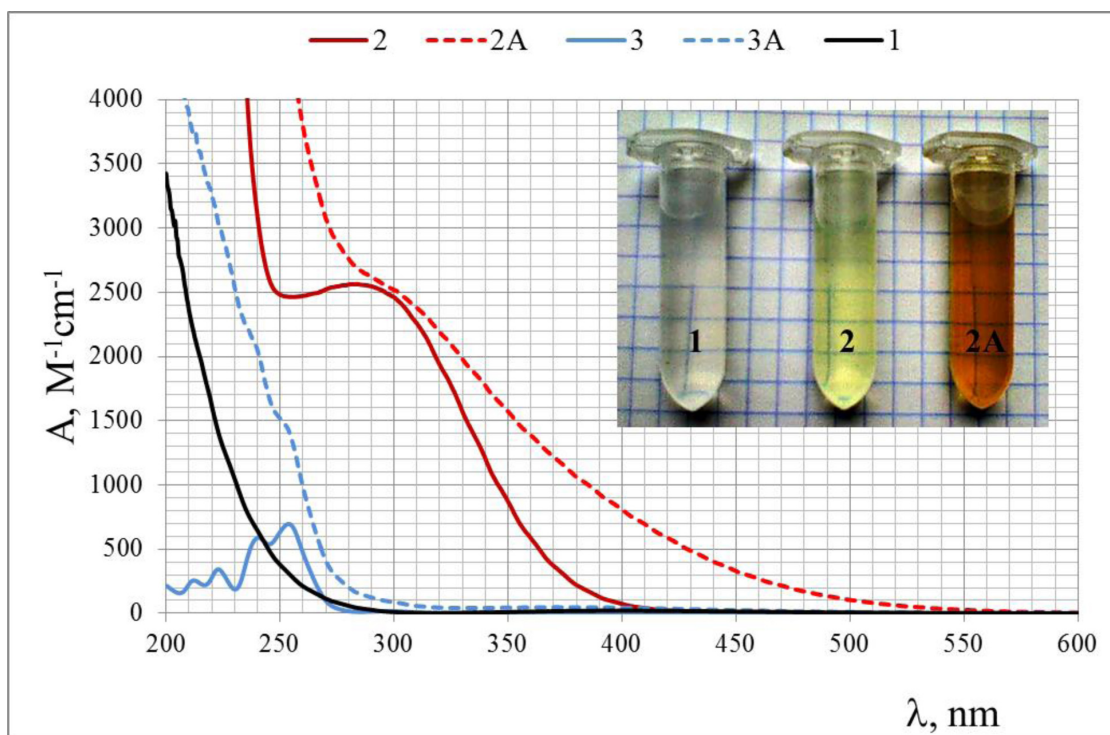
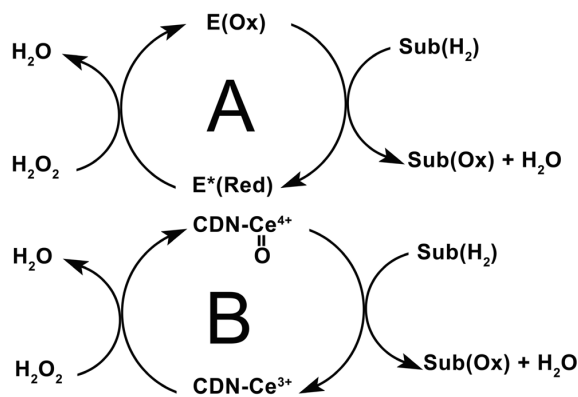


FIG. 7. Absorption spectra of hydrogen peroxide (1),  $(\text{NH}_4)_2\text{Ce}(\text{NO}_3)_6$  aqueous solution before (2) and after injection of  $\text{H}_2\text{O}_2$  (2A) and  $\text{CeCl}_3$  aqueous solution before (3) and after (3A) injection of equimolar quantity of  $\text{H}_2\text{O}_2$ . Inset: Appearance of corresponding solutions

grape) [43]. There, it was shown that the balance of pro-oxidant and anti-oxidant properties of CDNs is dependent on the pH. A detailed study of the peroxidase activity of CDNs (including Michaelis–Menten constants) justified the possibility for the replacement of horseradish peroxidase (HRP) by cerium dioxide sols for the oxidation of the substrate (3,3,5,5-tetramethylbiphenyl dihydrochloride) in a glucose test [44]. It was shown for  $\text{H}_2\text{O}_2$ -substrate that the maximal reaction rate in the presence of CDNs exceeds the similar value for HRP ( $5.07 \cdot 10^{-8} \text{ M} \cdot \text{s}^{-1}$  and  $3.34 \cdot 10^{-8} \text{ M} \cdot \text{s}^{-1}$ , accordingly).

Scheme 5(A) shows a simplified catalytic cycle of peroxidase; here,  $\text{E}^*(\text{Red})$  and  $\text{E}(\text{Ox})$  are reduced and oxidized forms of the enzyme, while  $\text{Sub}(\text{Red})$  and  $\text{Sub}(\text{Ox})$  are reduced and oxidized forms of the substrate, respectively. As well as in the case of oxidase mimetic, the decrease in pH enhances pro-oxidant properties of  $\text{CeO}_2$  and raises the reaction rate under Scheme 5B (right part), but the possibility of the particles' regeneration under Scheme 5(B, left part) drops. It is obvious that for peroxidase-like activity of CDNs (as in the case of oxidase mimetic) there should be also an optimum pH value, located in the acidic area. For instance, Jiao *et al.* [44] also show that peroxidase-like activity of CDNs is maximal at pH 4, while at pH  $< 2$  and pH  $> 6$  it is lost. As mentioned above, at high pH values, nanocrystalline cerium dioxide exhibits catalase mimetic activity.



Scheme 5. Peroxidase-like activity of CDN

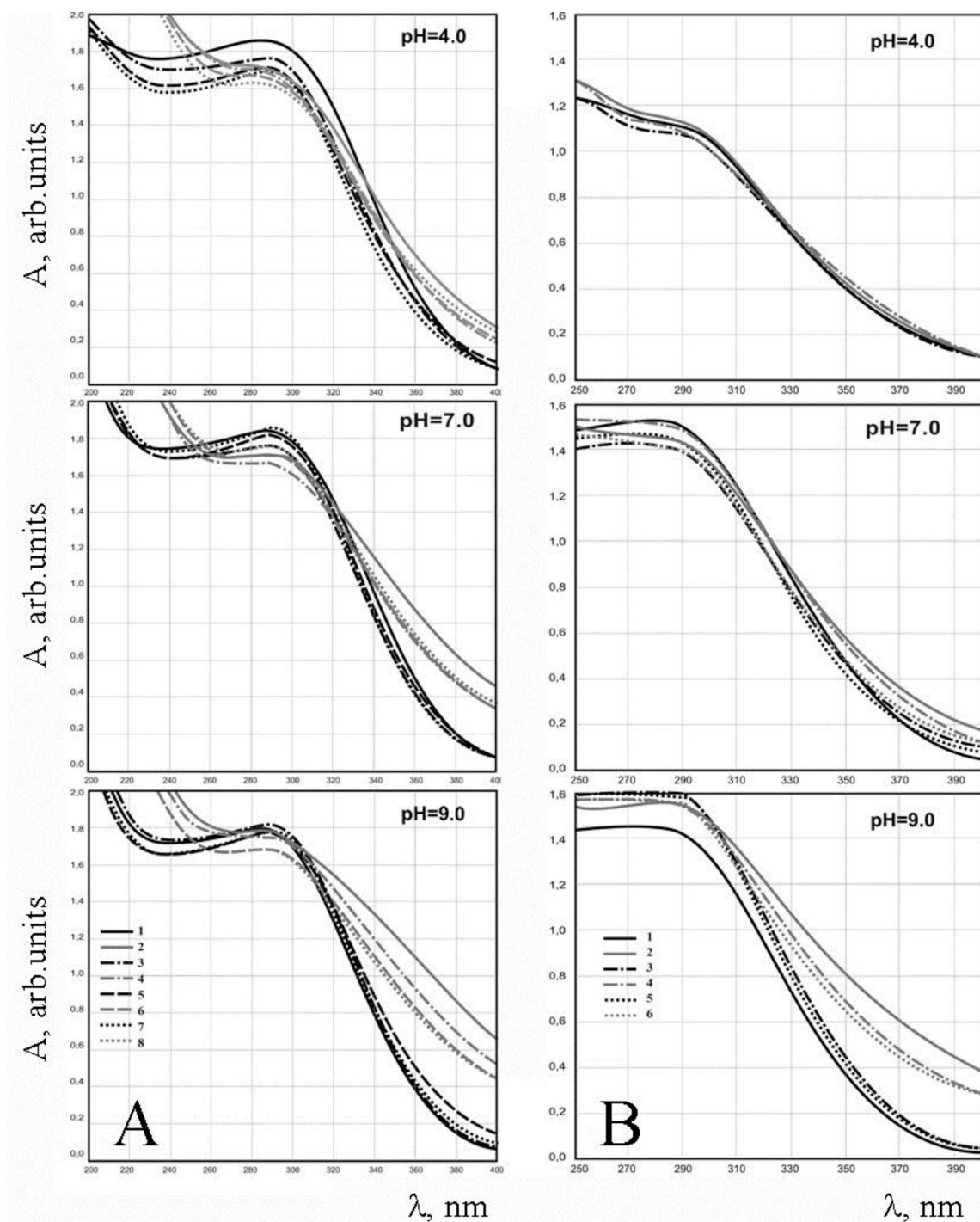


FIG. 8. Regeneration of 0.5 mM CeO<sub>2</sub> sol in alkaline, neutral and acidic media upon treatment by hydrogen peroxide: 1 – initial CeO<sub>2</sub> sol; 2 – injection of 1 mM H<sub>2</sub>O<sub>2</sub>; 3 – boiling for 5 minutes; 4 – injection of additional 1 mM H<sub>2</sub>O<sub>2</sub>; 5 – additional boiling for 5 minutes; 6 – injection of additional 1 mM H<sub>2</sub>O<sub>2</sub>; 7 – additional boiling for 5 minutes; 8 – injection of additional 1 mM H<sub>2</sub>O<sub>2</sub>. A – the data for citrate-stabilized ceria sol containing 2–3 nm particles; B – the data for polyacrylate-stabilized ceria sol containing 4–5 nm particles

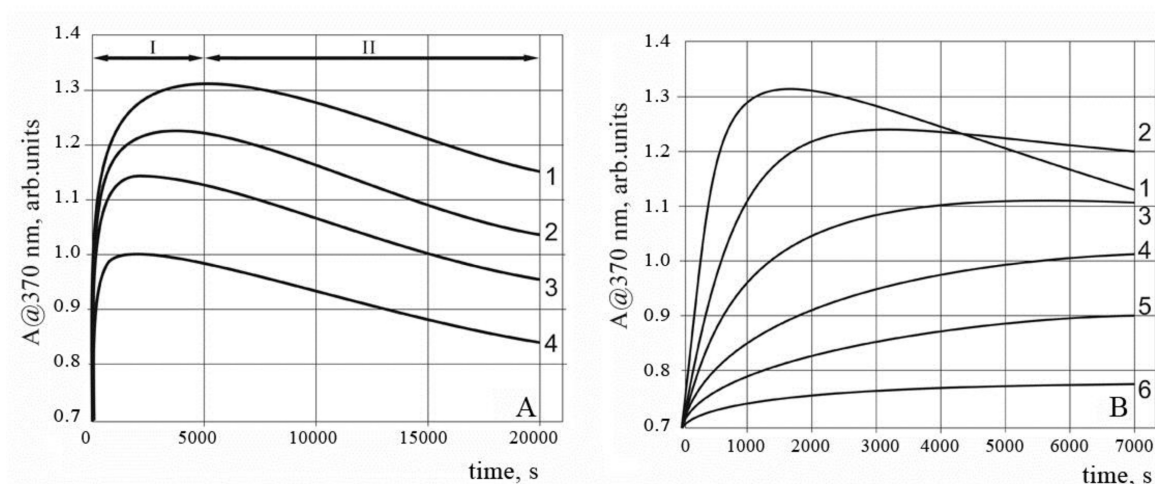


FIG. 9. (A) Dynamics of optical density change at 370 nm wavelength of 400  $\mu\text{M}$  aqueous colloid solution of  $\text{CeO}_2$  nanoparticles upon injection of hydrogen peroxide of different concentrations: 1 – 400  $\mu\text{M}$ ; 2 – 200  $\mu\text{M}$ ; 3 – 100  $\mu\text{M}$ ; 4 – 50  $\mu\text{M}$  (pH 80). (B) Dynamics of optical density change at 370 nm wavelength of 400  $\mu\text{M}$  aqueous colloid solution of  $\text{CeO}_2$  nanoparticles upon injection of hydrogen peroxide at different pH values: 1 – pH 9; 2 – pH 8; 3 – pH 7; 4 – pH 6; 5 – pH 5; 6 – pH 4 (concentration of  $\text{H}_2\text{O}_2$  is 200  $\mu\text{M}$ )

Pro- and anti-oxidant properties of CDNs are closely related and determined by several key factors. Let us consider the role of CDNs in the oxidation of indigoid dyes by hydrogen peroxide as an example. Indigo carmine is decomposed by ROS in the whole range of pH (Fig. 10). In the presence of nanoceria (particle size 3–5 nm, stabilized by citrate,  $\zeta$ -potential of about  $-20$  mV), the oxidation rate of indigo carmine by  $\text{H}_2\text{O}_2$  is changed: at pH  $<6$ , the rate of dye degradation by hydrogen peroxide is enhanced, i.e. CDNs exhibit peroxidase-like activity. Contrarily, at pH  $>7$  the rate of discoloration of the solution decreased, thus revealing the catalase-like activity of CDNs (Fig. 11).

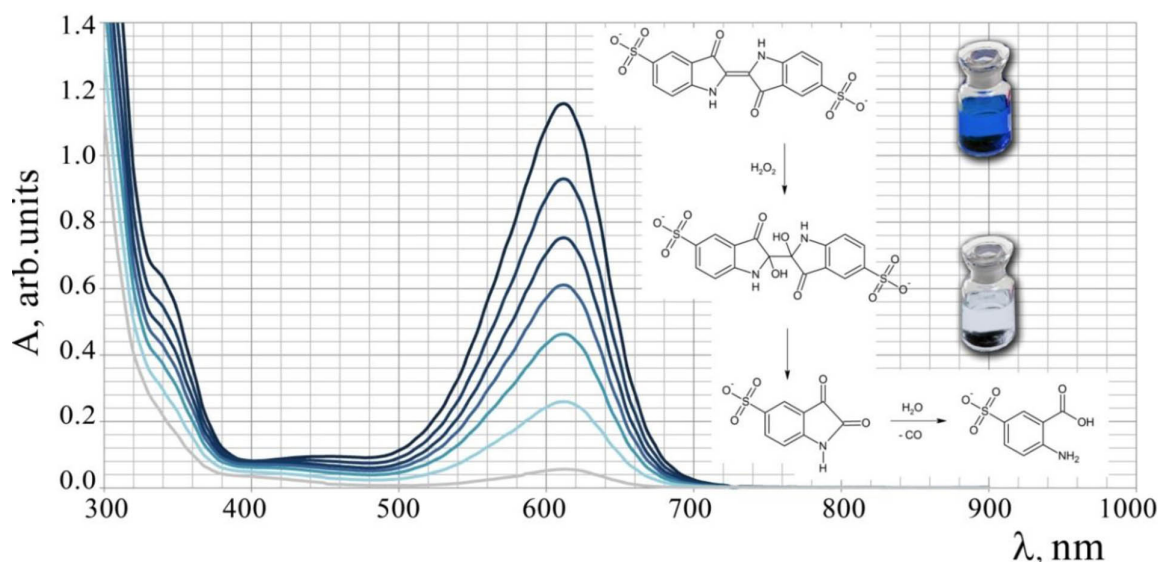


FIG. 10. The kinetics of indigo carmine dye solution (75  $\mu\text{M}$ ) decomposition in the presence of hydrogen peroxide (1 mM), and scheme of the corresponding process

The ability of  $\text{CeO}_2$  to decompose hydrogen peroxide can also be described in terms of its electrochemical behavior in aqueous solutions. The standard electrode potential ( $E^\circ$ ) for  $\text{CeO}_2/\text{Ce}^{3+}$  is 1.66 V; for  $\text{O}_2/\text{H}_2\text{O}_2$   $E^\circ$  it is 0.695 V [25].

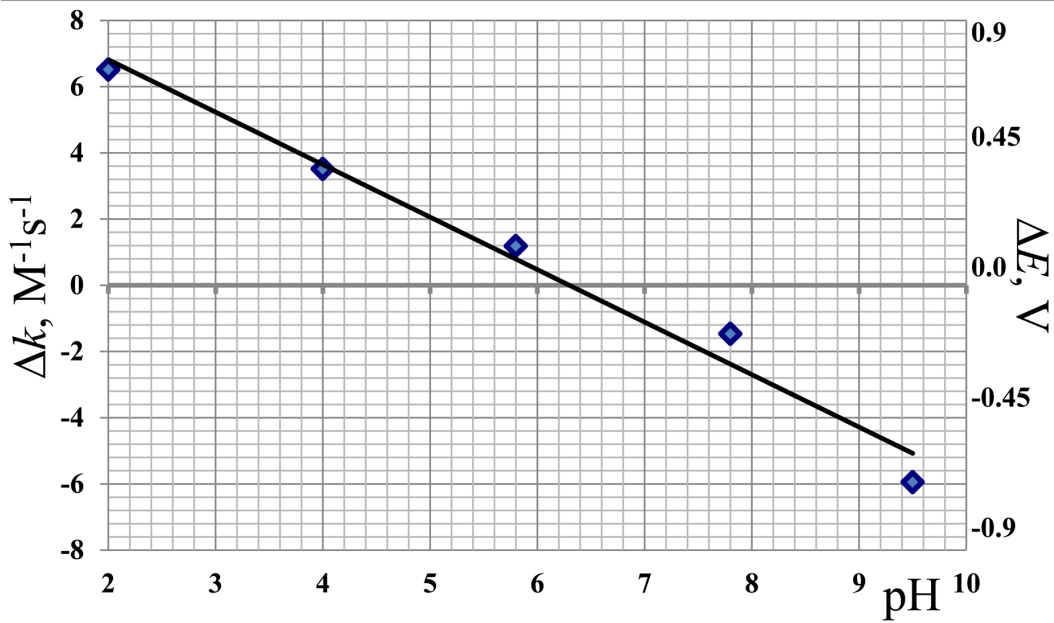


FIG. 11. Square dots denote changes of the rate constant of indigo carmine dye ( $75 \mu\text{M}$ ) discoloration by hydrogen peroxide ( $1 \text{ mM}$ ) caused by the introduction of CDNs ( $50 \mu\text{M}$ ) as a function of pH (left axis). The solid line is the calculated difference between the redox potentials of CDNs and hydrogen peroxide as a function of pH (right axis)

In accordance with the Nernst equation, for  $\text{Ce}^{3+} + 2\text{H}_2\text{O} \rightarrow \text{CeO}_2 + 4\text{H}^+ + \text{e}^-$  reaction the redox potential depends on pH, as follows:

$$E1 = 1.66 + 2.3 \frac{RT}{nF} \left( \log \left( \frac{[\text{CeO}_2]}{[\text{Ce}^{(3+) }]} \right) - 4pH \right) = 1.66 + 0.05916 \left( \log \left( \frac{[\text{CeO}_2]}{[\text{Ce}^{(3+) }]} \right) - 4pH \right).$$

Redox potential of  $\text{H}_2\text{O}_2 \rightarrow \text{O}_2 + 2\text{H}^+ + 2\text{e}^-$  reaction depends on the pH as:

$$E2 = 0.695 + 2.3 \frac{RT}{nF} \left( \log \left( \frac{p_{\text{O}_2}}{[\text{H}_2\text{O}_2]} \right) - 2pH \right) = 0.695 + 2.3 \frac{RT}{2F} \left( \log \left( \frac{p_{\text{O}_2}}{[\text{H}_2\text{O}_2]} \right) - 2pH \right) = 0.695 + 0.02958 \left( \log \left( \frac{p_{\text{O}_2}}{[\text{H}_2\text{O}_2]} \right) - 2pH \right).$$

Therefore, if  $E1 < E2$  or

$$1.66 + 0.05916 \left( \log \left( \frac{[\text{CeO}_2]}{[\text{Ce}^{(3+) }]} \right) - 4pH \right) < 0.695 + 0.02958 \left( \log \left( \frac{p_{\text{O}_2}}{[\text{H}_2\text{O}_2]} \right) - 2pH \right),$$

then nanoceria reduces hydrogen peroxide (i.e. it acts as an anti-oxidant and protects from hydrogen peroxide). This condition is satisfied when  $pH > 5.6 - \frac{1}{3} \left( \log(D) - \frac{1}{2} \log[\text{H}_2\text{O}_2] \right)$ . We assume that  $p_{\text{O}_2} = 0.1$  and denotes the mole fraction of Ce(III) in the particle as  $D$  (since cerium dioxide is insoluble there are no cerium ions present in the solution).

The total concentration of hydrogen peroxide above  $\approx 1 \text{ mM}$  causes cell death in mammals. The decomposition of the hydrogen peroxide to a lower concentration will occur at  $pH \geq 5.1 - \frac{1}{3} \log(D)$ .

In stoichiometric coarse-grained  $\text{CeO}_2$ , trivalent cerium ions are almost absent ( $D \leq 10^{-8}$ ). For such material, the limiting value is  $pH > 5.1 - \log(10^{-8}) = 7.77$ . In other words, at  $pH < 7.8$ , stoichiometric cerium dioxide could not function as an anti-oxidant against hydrogen peroxide (because in this pH range the redox potential of ceria is higher than that of  $\text{H}_2\text{O}_2$ ). In non-stoichiometric cerium dioxide (especially in the presence of organic stabilizer), the  $D$  value reaches 0.01–0.001 and above [45]. For  $\text{CeO}_2$  with  $D = 0.001$ , the threshold pH value is  $pH > 5.1 - \log(10^{-3}) = 6.1$ . In other words, at  $pH > ca. 6$ , non-stoichiometric ceria is able to protect biological systems and their components from hydrogen peroxide.

Figure 11 shows the dependence of the difference between the redox potentials of CDNs ( $D = 0.001$ ) and  $1 \text{ mM}$  of hydrogen peroxide ( $\Delta E = E1 - E2$ ) from the pH of media (solid line). The difference between the rate

constants of indigo carmine dye decomposition by hydrogen peroxide in the absence and the presence of nanoceria is also shown as square dots ( $\Delta k = k_1 - k_2$ ). This straight line coincides with the trend of the kinetic constant change of indigoid dye oxidation by hydrogen peroxide that is caused by ceria introduction.

The proposed calculation allows one to evaluate the protective ability of various cerium dioxide particles against ROS (e.g. hydrogen peroxide), taking into account the pH value of the medium in cells or cell organelles [46]. The respective data obtained for stoichiometric and non-stoichiometric cerium dioxide specimens are shown in Fig. 12. Alteration of the stoichiometry can be used to control pro- or anti-oxidant properties of CDNs across a wide range of biologically relevant pH values. As can be seen from the figure, the minimum protection against oxidation is observed for the content of some vesicles (lysosomes and endosomes). It is well known that in eukaryotes, most of the substances are transported into cells via vesicular uptake mechanisms. Endocytosis provides a path for the useful nutrients (such as proteins, nucleic acids, polysaccharides and lipoprotein complexes) as well as the undesirable species (such as toxins, antibodies and virions, etc.). The oxidizing properties of CDNs may be useful for the destruction of dangerous exogenous components in the course of the vesicular transportation of nutrients into the cells. On the other hand, the analysis of pH-dependent redox behavior of CDNs suggests that the maximum protection from oxidative stress is manifested in the mitochondria. As is known, the endogenous oxidative processes in cells take place in mitochondria; they are actively involved in the generation of ROS and participate in the cascade of the programmed cell death. There is a proven correlation between excessive mitochondrial generation of ROS and aging [47]. Mitochondria-targeted anti-oxidants are effective protectors of cells and their organelles, under the conditions of oxidative stress or aging [48].

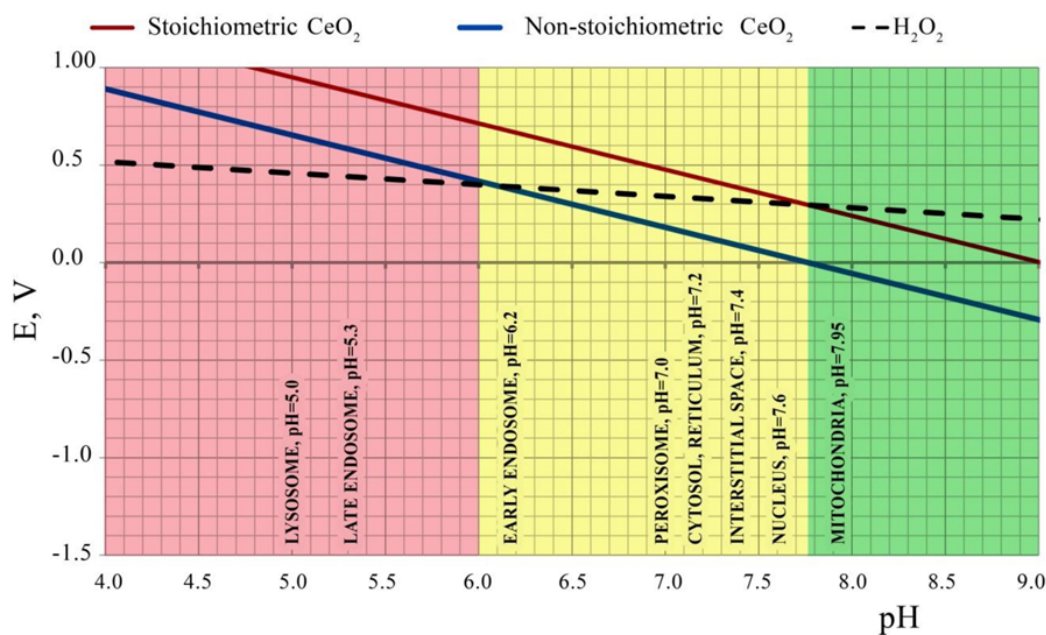


FIG. 12. E-pH diagram for hydrogen peroxide and stoichiometric and non-stoichiometric  $\text{CeO}_2$ . The cellular organelles with the corresponding pH values are shown along the absciss

Figure 12 demonstrates that the CDN's behavior strictly depends on its stoichiometry, even in similar biological experiments. For example, recently we have demonstrated that ceria nanoparticles (2–5 nm) protect against oxidative stress in murine oocytes and boost their activity [49], while authors [50] have found that cerium dioxide nanoparticles of the same size ( $\sim 3$  nm) are pro-oxidants for murine oocytes and invoke oxidative damage of DNA. In the first case, nanoparticles have been obtained from salts of cerium (III) under “mild conditions” and contained more than 15 %  $\text{Ce}^{3+}$  [45]; in the second case nanoparticles (Rhodia) have been synthesized from cerium (IV) salts and practically did not contain  $\text{Ce}^{3+}$  (less than 0.04 %) [51].

From the point of view of nanopharmaceutics, a pH-dependent equilibrium of pro- and anti-oxidant properties of the CDNs is of great interest; it could be applied for the development of antiviral drugs, for instance. Most viruses penetrate cells via endocytosis. The agglutination and release of genetic material require a low pH in vesicles. Thus, influenza hemagglutinin is inactive at pH 7. Fusion peptides change their conformation in acidic media only (at  $\text{pH} \leq 5$ ). At this pH, nanocrystalline cerium dioxide exhibits pro-oxidant properties, and thus can damage the nucleic acids of the virion. In vitro experiments revealed that CDNs (particles size 3–5 nm,

stabilized with citrate,  $\zeta$ -potential of about  $-20$  mV, concentration of  $0.01$ – $0.1$  mM) provide virus-resistance both in prophylactic and therapeutic (1 h after infecting) schemes, and also demonstrate a significant virucidal effect, reducing the titer of RNA virus (vesicular stomatitis) and DNA virus (herpes simplex type 1) in L929 and RF cells by  $2.6$ – $4.8$  lg [52]. The selectivity index (the ratio of the effective antiviral and cytotoxic doses) is more than  $16.0$ , which is typical for active antiviral drugs.

The prospect of the application of nanoceria for the redox treatment of tumours is even more exciting. Due to anaerobic respiration that occurs in the cytosol (lactic acid fermentation), rather than oxidative phosphorylation in the mitochondria (the Warburg effect), cancer cells express increased glycolysis. It is known that the pH value of the medium in a tumor is decreased (Fig. 13 [53]). Further, the tumor exists in a state of hypoxia permanently, and the partial oxygen pressure in the carcinogenesis area is also decreased [54]. For the calculation of pH-dependent redox activity (see above) of CDNs in normal tissue  $p_{O_2} \approx 0.1$  was used. The partial pressure of oxygen in tumors may be in the range of  $p_{O_2} \approx 0.01 - 0.001$ , therefore the redox activity of CDNs towards ROS (hydrogen peroxide) would be observed at  $0.2$ – $0.4$  pH points higher than in normal tissue. Thus,  $CeO_2$  nanoparticles can selectively protect the normal cells (unlike malignant cells) from oxidative stress.

The pioneering experiments with oxidative destruction of normal tissue cells (cardiomyocytes and fibroblasts) and tumor cells (lung carcinoma and breast cancer) substantiated this assumption [42]. Our latest experiments confirm it also: according to the data presented in paper [55], panthenol-stabilized non-stoichiometric cerium dioxide nanoparticles provide strong protection for both normal (diploid epithelial swine testicular, ST) and malignant (human epidermoid cancer, HEP-2) cells under oxidative stress conditions induced by UV irradiation. However, the degree of protection against  $H_2O_2$ -induced oxidative stress dramatically differs: the application of  $63 \mu M$   $CeO_2$  sols increases the viability of malignant cells not more than  $10$ – $15$  % over negative control ( $H_2O_2$ ), while the same concentration of the  $CeO_2$  protects normal cells almost completely (Fig. 14).

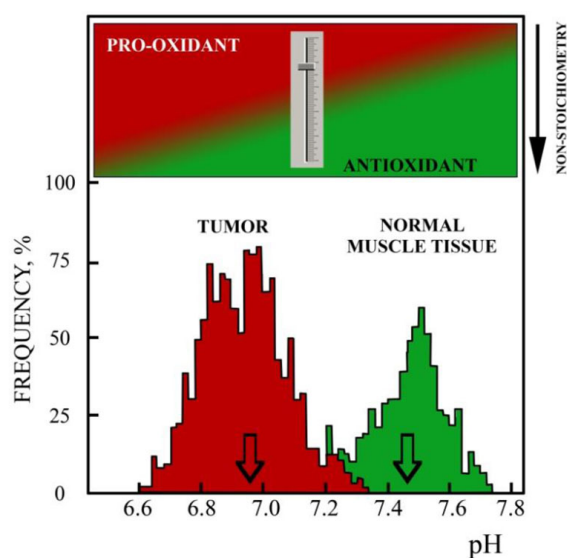


FIG. 13. Bottom: average frequency of measured pH values in the area of SCK-cells in carcinoma and normal muscle tissue in mice [53]. Top: pro-oxidant and anti-oxidant properties of the  $CeO_2$  nanoparticles of various stoichiometry and the possibility of fine-tuning of such properties in the given pH range (see Fig. 12)

Usually, seriously damaged cells undergo programmed cell death (apoptosis), a mechanism of self-destruction that involves mitochondria, but this mechanism fails in cancer cells. It was shown that  $20$  nm ceria nanoparticles in the concentrations of  $3.5$ ,  $10.5$  and  $23.3 \mu g/ml$  after  $24$ ,  $48$  and  $72$  h exposure had an oxidative effect on A549 human lung cancer cells [56]. Cell viability was reduced proportionally to the administered dose of nanoparticles and the duration of the exposure. In the whole range of studied concentrations, the nanoparticles induced oxidative stress. The concentrations of glutathione and  $\alpha$ -tocopherol were reduced, whilst the concentrations of malondialdehyde and lactate dehydrogenase, evidencing lipid peroxidation and cell membrane damage, were increased. The authors [57] showed that CDNs reduce viability of SMMC-7721 human hepatoma cells by inducing the apoptosis via the oxidative stress mechanism.  $CeO_2$  nanoparticles significantly increase the production of ROS and simultaneously reduce the activity of superoxide dismutase, glutathione peroxidase and catalase.

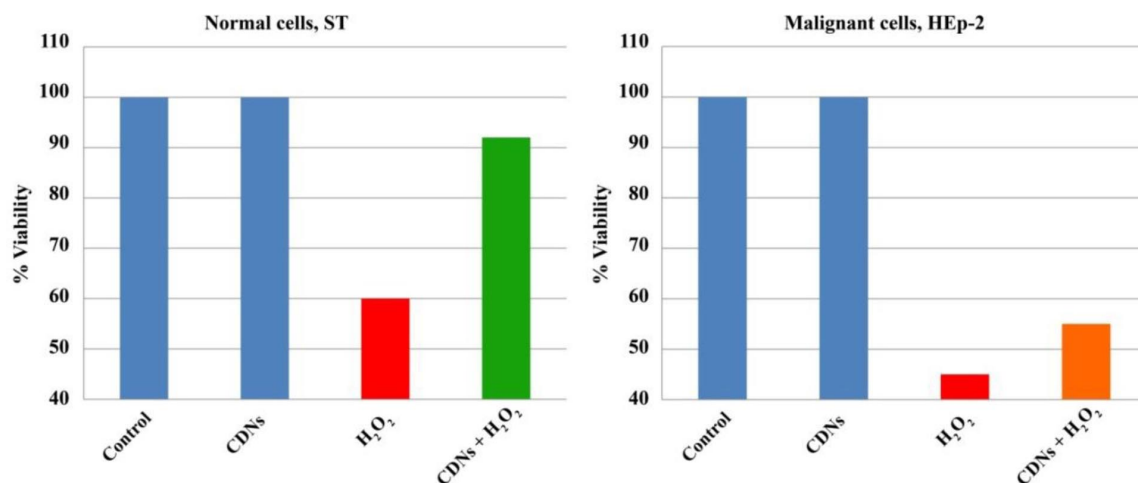


FIG. 14. The number of surviving diploid epithelial swine testicular (ST) and human epidermoid cancer (HEp-2) cells under the following conditions (left to right): control, in the presence of  $63 \mu\text{M}$  cerium dioxide nanoparticles, in the presence of  $0.5 \text{ mM}$  hydrogen peroxide, in the presence of  $0.5 \text{ mM}$  hydrogen peroxide and  $63 \mu\text{M}$  cerium dioxide nanoparticles [55]

Melanoma is the most aggressive type of skin cancer that is caused by the uncontrolled proliferation of melanocytes. Melanoma cells are highly metastatic and treatment of melanoma is ineffective, due to its high resistance to conventional chemotherapy. The authors investigated the inhibition of human melanoma cells (A375) by CDNs *in vitro* and *in vivo* in immunodeficient mice [58]. Unstabilized  $\text{CeO}_2$  nanoparticles and nanoparticles coated with dextran were used in the experiments. According to the authors,  $\text{Ce}^{3+}/\text{Ce}^{4+}$  ratio in the particles was 67/33 and 21/79 respectively. It was found that nanoparticles were not toxic to stromal cells (fibroblasts and endothelial cells) in all the studied concentrations. However, in the presence of nanoparticles, the viability of tumor cells was significantly decreased. Inhibition of melanoma cells' activity was proportional to the applied concentration of ceria nanoparticles and the duration of exposure. Analysis of the oxidative stress and apoptosis indicators showed that the presence of CDNs caused oxidative stress in cancer cells, resulting in their lower viability and reduced proliferation. The authors showed that CDNs (particle size 3–5 nm, dextran-stabilized) had a cytotoxic effect on SCL-1 carcinoma tumor cells and also reduced their proliferation [59]. Simultaneously, CDNs were non-toxic to the stromal cells and were capable of protecting normal (non-malignant) human dermal fibroblasts from oxidative stress.  $\text{CeO}_2$  nanoparticles (with a size of about 100 nm) were synthesized by two different techniques [60]. In the first case, the particles were annealed at  $800 \text{ }^\circ\text{C}$  at the final step of the synthesis, whilst in the second case, the particles in the solution were heated up to a temperature of  $60 \text{ }^\circ\text{C}$ . The first type of particles was presumably free of trivalent cerium, whereas the particles of the second type contained  $\text{Ce}^{3+}$  on the surface. The particles without trivalent cerium were slightly more toxic to the normal cells of the L929 line and significantly more toxic to PC-3 prostate cancer cells.

The study of parameters affecting the redox-properties of cerium dioxide will allow the designing of the ceria-based nanozymes for required biochemical processes. CDNs with a high level of non-stoichiometry protect both normal and malignant cells against ROS, whilst the stoichiometric CDNs could serve as pro-oxidants for both types of cells, as can be seen from Fig. 12 and Fig. 13. There is also a transient area between these two extremities:  $\text{CeO}_2$  nanoparticles of a certain size and stoichiometry are capable of providing a selective protection in normal cells, and serve as an oxidative stress promoter in malignant cells. We have developed several techniques for the synthesis of ceria preparations with the desired physical and chemical parameters ("fine tuning", see Fig. 13). Examples of such preparations are the sols of cerium dioxide, stabilized by low molecular weight glucans [29,61]. The protective effects of thus prepared cerium dioxide particles, such as inactivation of the hydroxyl radicals or protection of cells against hydrogen peroxide, depend on the size of the particles, which in turn depends on the cerium/glucose ratio in the precursor's mixture [29]. It should be noted that hypoxia and the decrease of pH in tumors is caused by the enhanced aerobic glycolysis, where tumors "trap" glucose [54]. It is expected that a CDN-glucan composite is to have an enhanced affinity towards cancer cells. Furthermore, due to the glucose presence, such a composite would accelerate hypoxia and decrease the pH, whilst simultaneously enhancing the oxidative stress in tumor cells.

Absence of specificity of chemical drugs to cancer cells is the basic problem of oncology. Ceria-based selective protection from oxidative stress opens new frontiers in the redox treatment of malignant tumors [62–64].

### 7. CDN can destroy nitrogen radicals

Cerium dioxide nanoparticles are able to inactivate nitrogen-containing free radicals, including reactive nitrogen species (RNS). RNS act together with ROS to damage cells, causing nitrosative stress. Dowding *et al.* [65] have demonstrated the activity of CeO<sub>2</sub> particles against the nitrosyl (short-lived nitroxyl) radical (\*NO). We have reported that nanocrystalline cerium dioxide also inactivates the stable nitroxyl radical (2,2,6,6-tetramethyl-4-piperidone-N-oxyl) [66]. Two types of CeO<sub>2</sub> nanoparticles were studied: 1–2 nm (stabilized by sodium citrate) and 3–5 nm (stabilized by sodium adenosine triphosphate). Interestingly, the inactivation rate was dependent on the particle size of CeO<sub>2</sub>, where it increased proportionally as the particle size decreased. As the particle size decreases, Ce<sup>3+</sup>/Ce<sup>4+</sup> ratio increases, so obviously trivalent cerium is crucial for the inactivation of radicals. Oxidation of Ce<sup>3+</sup> during nitroxyl inactivation suggests that cerium oxide nanoparticles adopt the NO-reductase function and possibly serve as an electron donor. Dowding *et al.* [67] have shown the ability of CDNs to scavenge a highly reactive molecule of peroxyxynitrite (ONO<sub>2</sub><sup>-</sup>). The rate of inactivation was independent of the Ce<sup>3+</sup>/Ce<sup>4+</sup> ratio on the surface of the particles, but was significantly reduced in the inert atmosphere.

### 8. CDN as phosphatase mimetic

It was recently shown that nanosized cerium oxide, which is capable of acting as oxidoreductases, could also exhibit phosphatase activity [68]. For example, cerium oxide catalyses the cleavage of the ester bond in the organic phosphoric acid esters, such as p-nitrophenyl phosphate, adenosine triphosphate, o-phospho-L-tyrosine, etc. The initial reaction rate increases with the decrease in the pH. The pre-oxidation of nanoceria by hydrogen peroxide leads to the decrease in the concentration of Ce<sup>3+</sup> and also to the drastic decrease of the dephosphorylation reaction rates. A plausible mechanism of the phosphatase activity of CDNs can be studied by using the hydrolysis of p-nitrophenyl phosphate (NPP), which is a standard substrate for testing serum alkaline phosphatase. In the presence of the enzyme or CDNs the colourless NPP releases the phosphate group forming p-nitrophenol, which has a bright yellow colour in the alkaline medium (see Fig. 15). The figure also shows the plausible mechanism of CDNs' catalysis of the dephosphorylation of the organic compounds. The comparison of the simplified mechanism of phosphatase (Scheme 6(A)) and CDN (B) action shows that nanocrystalline cerium dioxide could hardly be called a phosphatase analog, since phosphate groups bind to cerium ions irreversibly. However, cerium phosphate is shown to be eliminated from the CeO<sub>2</sub> particle, resulting in the regeneration of its surface. The renewed particle could repeatedly take part in the reaction (similar to the enzyme) until the complete disappearance of the particle.

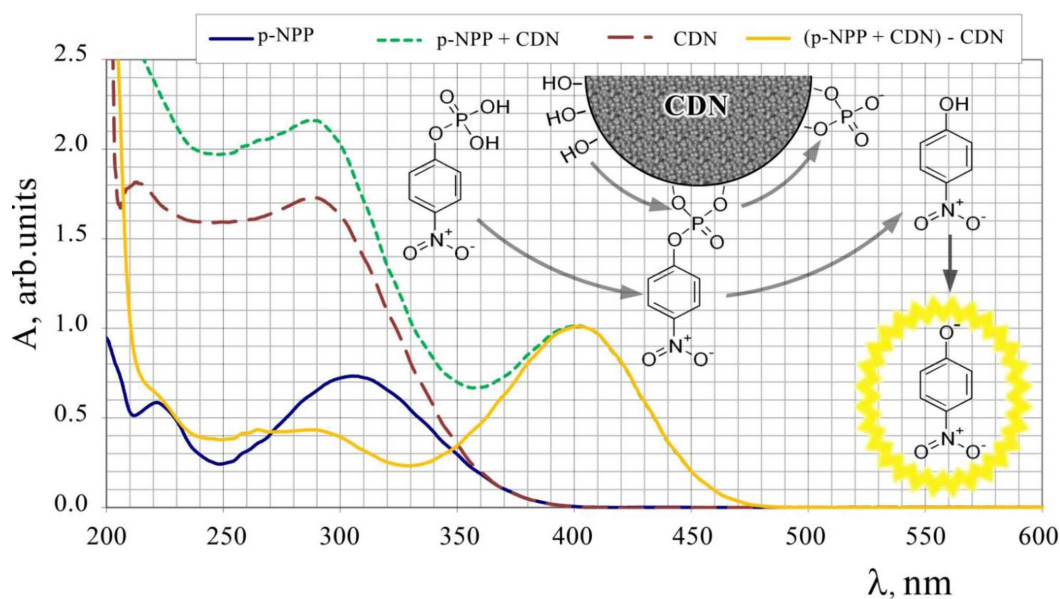
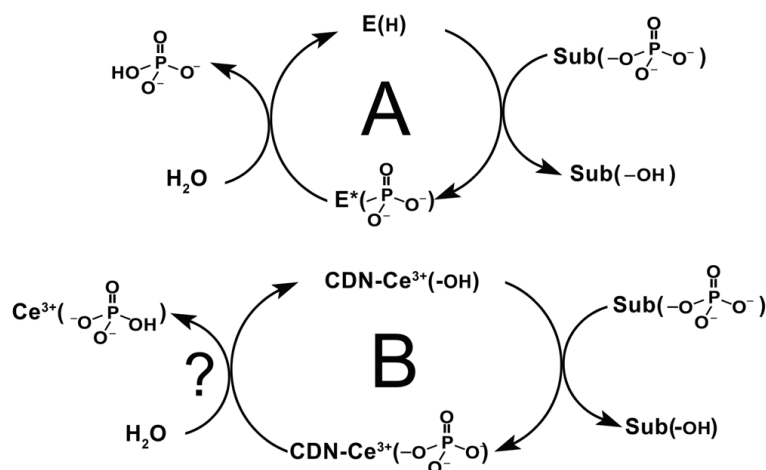


FIG. 15. The absorption spectra of p-nitrophenylphosphate (50 mM) before and after adding of CDNs (500 μM) at pH 7.8. Inset: Proposed mechanism of dephosphorylation of organic compounds in the presence of CDN



Scheme 6. CDN showing phosphatase-like activity

Jia *et al.* [69] used nanosized cerium dioxide for concentrating and quantitative dephosphorylation of phosphopeptides. Park *et al.* [70] reported that nanosized cerium oxide can initiate the phosphorylation of the mitogen-activated protein kinase in human bronchial epithelial cells (Beas2B).

The activation of the transcription factor NF- $\kappa$ B depends on the phosphorylation of the protein-inhibitor by I $\kappa$ B $\alpha$  kinases (IKK). NF- $\kappa$ B is involved in inflammatory processes and is activated by the external physical or chemical factors (radiation, ultraviolet light or toxins), infectious agents (bacteria, viruses, parasites and their metabolic products), or by the signal molecules etc. Hyperactivation of the NF- $\kappa$ B leads to the synthesis of a number of pro-inflammatory cytokines, such as the family of interleukins, the tumour necrosis factor (TNF- $\alpha$ ), the  $\gamma$ -interferon and macrophages activator, etc. Stress-kinase p38 activates the cascade of arachidonic acid, which is released from the phospholipids in the course of cell membrane lipid peroxidation, thus activating the cyclooxygenase, which is followed by the synthesis of inflammatory prostaglandins and lipoxygenase; it is then followed by the synthesis of leukotrienes – the mediators of the immediate-type allergic reaction. All these cascades have a pro-oxidant function and enhance the inflammatory response. The possibility of the targeted regulation of activity of the nuclear transcription factor is promising for a large number of pathological processes in the cell. For instance, the toxins in cigarette smoke extracts cause an inflammatory response in H9c2 cardiomyocytes. Pre-treatment of cells with CeO<sub>2</sub> nanoparticles (10 nM for 24 hours incubation prior to administration of 10% cigarette smoke extract) improves the survival of the cells' culture [71]. Biochemical studies have shown that nanoparticles inhibit phosphorylation of I $\kappa$ B $\alpha$ , thus reducing translocation of the p65 subunit, which is caused by the activation of NF- $\kappa$ B. Furthermore, the cells treated with cerium dioxide nanoparticles have reduced levels of some interleukins, e.g. tumor necrosis factor and inducible nitric oxide synthase (iNOS).

For their own replication, viruses use the signalling pathways and transcription factors of living cells. They activate IKK kinase; phosphorylation of the protein-inhibitor I $\kappa$ B causes the activation of the nuclear factor NF- $\kappa$ B; this activation increases the expression of viral genetic material. Conventional antiviral drugs do not affect IKK cascades. Simultaneously, the use of prostaglandin A<sub>1</sub>, which reduces the activity of IKK, results in a more than 3000-fold reduction of viral replication [72]. The development of effective drugs, inhibiting the phosphorylation of I $\kappa$ B, and their introduction into clinical practice, would open a new avenue in the treatment of viral infections [13]. Reversible phosphorylation and dephosphorylation reactions constitute the basis of the energy, metabolism and signalling pathways in cells. Phosphatase-like properties of ceria nanoparticles open a new way in assessing and predicting the biological activities of cerium oxide nanoparticles [73]. Probably, in the near future, there will be investigations into other biochemical processes that involve CDNs as a phosphatase (phosphate anion or organic phosphates acceptor). For example, the study of acetylcholinesterase reactivation by CDNs would be advantageous for the development of novel antidotes against the intoxication by organophosphorus compounds, etc.

## 9. Conclusions

CDN-based nanozymes are being widely used in nanopharmaceutical applications (such as development of the nanoscale techniques of chemical analysis, and development of the biomaterials for implants, which exhibit the desired therapeutic effect depending on the composition of blood development of molecular sensors and biosensors, etc. [74]). It should be noted that ceria's behavior in living systems and its unique biological activity and ability to perform the function of certain enzymes are determined by a number of factors, many of which are yet to be

established. The scope of application of nano-ceria is far from being restricted to the examples presented here. While the potential of CDNs as an active component of pharmaceuticals of the new generation is already evident, the development and clinical trials of ceria-based preparations will require further joint interdisciplinary efforts.

### Acknowledgments

This research has been supported by the Russian Science Foundation (project 17-73-10417).

### References

- [1] Kirby A.J. Enzyme Mechanisms, Models, and Mimics. *Angew. Chem.*, Int. Ed. 1996, **35**, P. 706–724.
- [2] Breslow R. *Artificial Enzymes and Enzyme Models*, in *Advances in Enzymology and Related Areas of Molecular Biology*, ed. A. Meister, John Wiley & Sons, Inc., Hoboken, NJ, USA, 1986, V. 58, pp. 1–60.
- [3] Schmuck C., Merschky M., Rether C., Geibel B. *Artificial Enzyme Mimics*, in *Supramolecular Chemistry: from Molecules to Nanomaterials*, ed. J.W. Steed and P.A. Gale, 2012.
- [4] Breslow R., Overman L.E., “Artificial enzyme” combining a metal catalytic group and a hydrophobic binding cavity. *J. Am. Chem. Soc.* 1970, **92**, P. 1075–1077.
- [5] Manea F., Houillon F.B., Pasquato L., Scrimin P. Nanozymes: Gold-Nanoparticle-Based Transphosphorylation Catalysts. *Angew. Chem.*, Int. Ed. 2004, **43**, P. 6165–6169.
- [6] Hu X.N., Liu J.B., Hou S., Wen T., Liu W.Q., Zhang K., He W.W., Ji Y.L., Ren H.X., Wang Q., Wu X.C. Research progress of nanoparticles as enzyme mimetics. *Sci. China Phys. Mech. Astron.*, 2011, **54**, P. 1749–1756.
- [7] Wei H., Wang E. Nanomaterials with enzyme-like characteristics (nanozymes): next-generation artificial enzymes. *Chem. Soc. Rev.*, 2013, **42**, P. 6060–6093.
- [8] Wang Z., Quan Z., Lin J. *Inorg. Chem.*, 2007, **46**, P. 5237.
- [9] Shcherbakov A.B., Ivanov V.K., Zholobak N.M., Ivanova O.S., Krysanov E.Y., Baranchikov A.E., Spivak N.Ya., Tretyakov Y.D. Nanocrystalline ceria based materials-Perspectives for biomedical application. *Biophysics*, 2011, **56**, P. 987–1004.
- [10] Ivanov V.K. Habil. Thesis, IGIC RAS of Moscow, 2011.
- [11] Ivanov V.K., Polezhaeva O.S., Shcherbakov A.B., Gil’ D.O., Tret’yakov Y.D. Microwave-hydrothermal synthesis of stable nanocrystalline ceria sols for biomedical uses. *Russ. J. Inorg. Chem.*, 2010, **55**, P. 1–5.
- [12] Ivanov V.K., Polezhaeva O.S., Shaporev A.S., Baranchikov A.E., Shcherbakov A.B., Usatenko A.V. Synthesis and thermal stability of nanocrystalline ceria sols stabilized by citric and polyacrylic acids. *Russ. J. Inorg. Chem.* 2010, **55**, P. 328–332.
- [13] Ivanov V.K., Shcherbakov A.B., Baranchikov A.E., Kozik V.V. *Synthesis, structure, physicochemical properties and biological activity of nanodispersed cerium dioxide*. Tomsk, Tomsk State University, 2013.
- [14] Ivanova O.S., Shekunova T.O., Ivanov V.K., Shcherbakov A.B., Popov A.L., Davydova G.A., Tret’yakov Y.D. One-stage synthesis of ceria colloid solutions for biomedical use. *Doklady Chem.*, 2011, **437**, P. 103–106.
- [15] Ivanov V.K., Shcherbakov A.B., Usatenko A.V. Structure-sensitive properties and biomedical applications of nanodispersed cerium dioxide. *Russ. Chem. Rev.*, 2009, **78**, P. 855–871.
- [16] Sun C., Xue D. Size-dependent oxygen storage ability of nano-sized ceria. *Phys. Chem.*, 2013, **15**(34), P. 14414–14419.
- [17] Tarnuzzer R.W., Colon J., Patil S., Seal S. Vacancy engineered ceria nanostructures for protection from radiation-induced cellular damage. *Nano Lett.*, 2005, **5**, P. 2573–2577.
- [18] Heckert E.G., Karakoti A.S., Seal S., Self W.T. The role of cerium redox state in the SOD mimetic activity of nanoceria. *Biomater.*, 2008, **29**, P. 2705–2709.
- [19] Karakoti A.S., Singh S., Kumar A., Malinska M., Kuchibhatla S.V.N.T., Wozniak K., Self W.T., Seal S. PEGylated nanoceria as radical scavenger with tunable redox chemistry. *J. Am. Chem. Soc.*, 2009, **131**, P. 14144–14145.
- [20] Korsvik C., Patil S., Seal S., Self W.T. Superoxide dismutase mimetic properties exhibited by vacancy engineered ceria nanoparticles. *Chem. Commun.*, 2007, P. 1056–1058.
- [21] Shcherbakov A.B., Ivanov V.K., Sirota T.V., Tret’yakov Y.D. Inhibition of adrenaline autooxidation by nanocrystalline ceria. *Doklady Chem.*, 2011, **437**, P. 60–62.
- [22] Klochkov V.K., Grigorova A.V., Sedyh O.O., Malyukin Yu.V. The influence of agglomeration of nanoparticles on their superoxide dismutase-mimetic activity. *Colloids Surf. A.*, 2012, **409**, P. 176–182.
- [23] Batinić-Haberle I., Rebouças J.S., Spasojević I. Superoxide dismutase mimics: chemistry, pharmacology, and therapeutic potential. *Antioxid. Redox Signal.*, 2010, **13**, P. 877–918.
- [24] Iranzo O. Manganese complexes displaying superoxide dismutase activity: A balance between different factors. *Bioorg. Chem.*, 2011, **39**, P. 73–87.
- [25] Yu P., Hayes S.A., O’Keefe T.J., O’Keefe M., Stoffer J.O. The phase stability of cerium species in aqueous systems II. The Ce(III/IV)-H<sub>2</sub>O-H<sub>2</sub>O<sub>2</sub>/O<sub>2</sub> systems. Equilibrium considerations and Pourbaix diagram calculations. *J. Electrochem. Soc.*, 2006, **153**, P. C74–C79.
- [26] Manda G., Nechifor M.T., Neagu T.-M. Reactive oxygen species, cancer and anti-cancer therapies. *Curr. Chem. Biol.*, 2009, **3**, P. 22–46.
- [27] Evans M.G., Uri N. Photo-oxidation of water by ceric ions. *Nature*, 1950, **166**(4223), P. 602–603.
- [28] Xue Y., Luan Q., Yang D., Yao X., Zhou K. Direct evidence for hydroxyl radical scavenging activity of cerium oxide nanoparticles. *J. Phys. Chem. C*, 2011, **115**, P. 4433–4438.
- [29] Shcherbakov A.B., Zholobak N.M., Ivanov V.K., Ivanova O.S., Marchevsky A.V., Baranchikov A.E., Tretyakov Y.D. Synthesis and antioxidant activity of biocompatible maltodextrin-stabilized aqueous sols of nanocrystalline ceria. *Russ. J. Inorg. Chem.*, 2012, **57**, P. 1411–1418.
- [30] Babu S., Velez A., Wozniak K., Szydłowska J., Seal S. Electron paramagnetic study on radical scavenging properties of ceria nanoparticles. *Chem. Phys. Lett.*, 2007, **442**, P. 405–408.
- [31] Asati A., Santra S., Kaitanis C., Nath S., Perez J.M. Oxidase-like activity of polymer-coated cerium oxide nanoparticles. *Angew. Chem. Int. Ed.*, 2009, **48**, P. 2308–2312.

- [32] Peng Y., Chen X., Yi G., Gao Z. Mechanism of the oxidation of organic dyes in the presence of nanocerium. *Chem. Commun.*, 2011, **47**, P. 2916–2918.
- [33] Pautler R., Kelly E.Y., Huang P.J.J., Cao J., Liu B., Liu J. Attaching DNA to nanocerium: Regulating oxidase activity and fluorescence quenching. *ACS Appl. Mater. Interfaces*, 2013, **5**, P. 6820–6825.
- [34] Makarov S.Z., Ladeinova L.V. Peroxy compounds of cerium. *Russ. Chem. Bull.*, 1961, **10**, P. 1091–1096.
- [35] Karakoti A.S., Munusamy P., Hostetler K., Kodali V., Kuchibhatla S., Orr G., Pounds J.G., Teeguarden J.G., Thrall B.D., Baer D.R. Preparation and characterization challenges to understanding environmental and biological impacts of nanoparticles. *Surf. Interface Anal.*, 2011, **44**, P. 882–889.
- [36] Floor M., Kieboom A.P.G., Van Bekkum H. *Recueil des Travaux Chimiques des Pays-Bas*. 1989, **108**, P. 128.
- [37] Rizkalla E.N., Lajunen L.H.J., Choppin G.R. Kinetics of the decomposition of hydrogen peroxide in the presence of ethylenediaminetetraacetatoceria(IV) complex. *Inorg. Chim. Acta.*, 1986, **119**, P. 93–98.
- [38] Heckert E.G., Seal S., Self W.T. Fenton-like reaction catalyzed by the rare earth inner transition metal cerium. *Environ. Sci. Technol.*, 2008, **42**, P. 5014–5019.
- [39] Halbhuer K.J., Hulstaert C.E., Feuerstein H., Zimmermann N. Cerium as capturing agent in phosphatase and oxidase histochemistry. Theoretical background and applications. *Prog. Histochem. Cytochem.*, 1994, **28**, P. 1–120.
- [40] Pirmohamed T., Dowding J.M., Singh S., Wasserman B., Heckert E., Karakoti A.S., King J.E., Seal S., Self W.T. Nanocerium exhibit redox state-dependent catalase mimetic activity. *Chem. Commun.* 2010, **46**, P. 2736–2738.
- [41] Das S., Dowding J.M., Klump K.E., McGinnis J.F., Self W., Seal S. Cerium oxide nanoparticles: applications and prospects in nanomedicine. *Nanomedicine*, 2013, **8**, P. 1483–1508.
- [42] Perez J.M., Asati A., Nath S., Kaittanis A. Synthesis of biocompatible dextran-coated nanocerium with pH-dependent antioxidant properties. *Small*, 2008, **4**, P. 552–556.
- [43] Ivanov V.K., Usatenko A.V., Shcherbakov A.B. Antioxidant Activity of Nanocrystalline Ceria to Anthocyanins. *Russ. J. Inorg. Chem.*, 2009, **54**, P. 1522–1527.
- [44] Jiao X., Song H., Zhao H., Bai W., Zhang L., Lv Y. Well-redispersed ceria nanoparticles: Promising peroxidase mimetics for H<sub>2</sub>O<sub>2</sub> and glucose detection. *Anal. Methods.*, 2012, **4**, P. 3261–3267.
- [45] Stoianov O.O., Ivanov V.K., Shcherbakov A.B., Stoyanova I.V., Chivireva N.A., Antonovich V.P. Determination of cerium(III) and cerium(IV) in nanodisperse ceria by chemical methods. *Russ. J. Inorg. Chem.*, 2014, **59**, P. 15–23.
- [46] Linnane A.W., Kios M., Vitetta L. Healthy aging: regulation of the metabolome by cellular redox modulation and prooxidant signaling systems: the essential roles of superoxide anion and hydrogen peroxide. *Biogerontology*, 2007, **8**, P. 445–467.
- [47] Finkel T., Holbrook N.J. Oxidants, oxidative stress and the biology of ageing. *Nature*, 2000, **408**(6809), P. 239–247.
- [48] Smith R.A., Murphy M.P. Mitochondria-targeted antioxidants as therapies. *Discov. Med.*, 2011, **11**, P. 106–114.
- [49] Shepel E.A., Zholobak N.M., Shcherbakov A.B., Antonovitch G.V., Yanchiy R.I., Ivanov V.K., Tretyakov Y.D. Ceria Nanoparticles Boost Activity of Aged Murine Oocytes. *Nano Biomed. Eng.*, 2012, **4**, P. 188–194.
- [50] Courbiere B., Auffan M., Rollais R., Tassistro V., Bonnefoy A., Botta A., Perrin J. Ultrastructural interactions and genotoxicity assay of cerium dioxide nanoparticles on mouse oocytes. *Int. J. Mol. Sci.*, 2013, **14**, P. 21613–21628.
- [51] Chane-Ching J.-Y. Cerium IV compound and method for its preparation. *Europ. Pat.* EP0208580 B1, 1990.
- [52] Zholobak N., Shcherbakov A., Ivanov V., Olevinskaya Z., Spivak N. Antiviral effectivity of ceria colloid solutions. *Antiviral Res.*, 2011, **90**, P. A67.
- [53] Song C.W., Griffin R., Park H.J. *Influence of tumor pH on therapeutic response*. In: *Cancer Drug Resistance*. ed. Teicher B.A. Humana Press, New Jersey, 2006, P. 21–42.
- [54] Osinsky S., Vaupel P. *Microphysiology of tumors*. Naukova dumka, Kiev, 2009.
- [55] Zholobak N.M., Shcherbakov A.B., Bogorad-Kobelska A.S., Ivanova O.S., Baranchikov A.Ye., Spivak N.Ya., Ivanov V.K. Panthenol-stabilized cerium dioxide nanoparticles for cosmetic formulations against ROS-induced and UV-induced damage. *J. Photochem. Photobiol. B*, 2014, **130**, P. 102–108.
- [56] Lin W., Huang Y.W., Zhou X.D., Ma Y. Toxicity of cerium oxide nanoparticles in human lung cancer cells. *Int. J. Toxicol.*, 2006, **25**, P. 451–457.
- [57] Cheng G., Guo W., Han L., Chen E., Kong L., Wang L., Ai W., Song N., Li H., Chen H. Cerium oxide nanoparticles induce cytotoxicity in human hepatoma SMMC-7721 cells via oxidative stress and the activation of MAPK signaling pathways. *Toxicol. Vitro*, 2013, **27**, P. 1082–1088.
- [58] Alili L., Sack M., von Montfort C., Giri S., Das S., Carroll K.S., Zanger K., Seal S., Brenneisen P. Downregulation of tumor growth and invasion by redox-active nanoparticles. *Antioxid. Redox Signal*, 2013, **19**, P. 765–778.
- [59] Alili L., Sack M., Karakoti A.S., Teuber S., Puschmann K., Hirst S.M., Reilly C.M., Zanger K., Stahl W., Das S., Seal S., Brenneisen P. Combined cytotoxic and anti-invasive properties of redox-active nanoparticles in tumor-stroma interactions. *Biomaterials*, 2011, **32**, P. 2918–2929.
- [60] Renu G., Divya V.V. Rani, Nair S.V., Subramanian K.R.V., Lakshmanan V.K. Development of cerium oxide nanoparticles and its cytotoxicity in prostate cancer cells. *Adv. Sci. Lett.*, 2012, **6**, P. 17–25.
- [61] Scherbakov A.B., Ivanov V.K., Zholobak N.M., Baranchikov A.E., Spivak N.Y., Ivanova O.S., Tretyakov Y.D. *Rus. Pat.* RU2012112921 C1, 2012.
- [62] Wondrak G.T. Redox-directed cancer therapeutics: Molecular mechanisms and opportunities. *Antioxid. Redox Signal*, 2009, **11**, P. 3013–3069.
- [63] McGinnis J.F., Wong L.L., Zhou X. Inhibition of neovascularization by cerium oxide nanoparticles, *US Pat.* US20090269410 A1, 2009.
- [64] Wason M.S., Zhao J. Cerium oxide nanoparticles: potential applications for cancer and other diseases. *Am. J. Transl. Res.*, 2013, **5**, P. 126–131.
- [65] Dowding J.M., Dosani T., Kumar A., Seal S., Self W.T. Cerium oxide nanoparticles scavenge nitric oxide radical (NO). *Chem. Commun.*, 2012, **48**, P. 4896–4898.
- [66] Ivanov V.K., Shcherbakov A.B., Ryabokon' I.G., Usatenko A.V., Zholobak N.M., Tretyakov Y.D. Inactivation of the nitroxyl radical by ceria nanoparticles. *Doklady Chem.*, 2010, **430**, P. 43–46.

- [67] Dowding J.M., Seal S., Self W.T. Cerium oxide nanoparticles accelerate the decay of peroxynitrite (ONOO<sup>-</sup>). *Drug Deliv. Transl. Res.*, 2013, **3**, P. 375–379.
- [68] Kuchma M.H., Komanski C.B., Colon J., Teblum A., Masunov A., Alvarado B., Babu S., Seal S., Summy J., Baker C.H. Phosphate ester hydrolysis of biologically relevant molecules by cerium oxide nanoparticles. *Nanomed. Nanotech. Biol. Med.*, 2010, **6**, P. 738–744.
- [69] Jia W., Andaya A., Leary J.A. Novel mass spectrometric method for phosphorylation quantification using cerium oxide nanoparticles and tandem mass tags. *Anal. Chem.*, 2012, **84**, P. 2466–2473.
- [70] Park E.J., Choi J., Park Y.K., Park K. Oxidative stress induced by cerium oxide nanoparticles in cultured BEAS-2B cells. *Toxicology*, 2008, **245**, P. 90–100.
- [71] Niu J.L., Wang K.K., Kolattukudy P.E. Cerium oxide nanoparticles inhibit oxidative stress and nuclear factor- $\kappa$ B activation in H9c2 cardiomyocytes exposed to cigarette smoke extract. *J. Pharmacol. Exp. Ther.*, 2011, **338**, P. 53–61.
- [72] Amici C., Belardo G., Rossi A., Santoro M.G. Activation of I $\kappa$ B kinase by herpes simplex virus Type 1. A novel target for anti-herpetic therapy. *J. Biol. Chem.*, 2001, **276**, P. 28759–28766.
- [73] Celardo I., Pedersen J.Z., Traversa E., Ghibelli L. Pharmacological potential of cerium oxide nanoparticles. *Nanoscale*, 2011, **3**, P. 1411–1420.
- [74] Rytting H. Pharmaceutical nanotechnology: A new section in IJP. *Int. J. Pharm.*, 2004, **281**, P. 1.